tin-activated dendritic cells express tumor necrosis factor superfamily, member 4 (OX40L), which initiates T-cell-mediated type 2 inflammation by activating OX40-positive T cells.[13] Upregulation of TSLP, TSLPR, and OX40L mRNA in RW-EAC models was reported by Zheng et al.[14] Interleukin-25 was originally discovered in cDNA libraries from highly polarized Th2 cells.[15] It is also produced by epithelial cells, mast cells, eosinophils, and macrophages.[3] The importance of IL-25 for type 2 inflammation was demonstrated by experiments using mouse OVA-induced asthma models, in which attenuated airway inflammation and airway hyperresponsiveness were observed after deletion of the IL-25 gene.[16] To date, there have been no published data concerning the expression of IL-25 in conjunctival tissue and its role in the pathophysiology of allergic conjunctivitis. In this study, we investigated the roles of type 2-initiating cytokines in the pathophysiology of allergic conjunctivitis by evaluating RW-EAC models by using IL-25 KO, IL-33 KO, and TSLPR KO mice and congenic wild-type mice.

Materials and Methods

IL-25 KO, IL-33 KO, and TSLPR KO Mice

Interleukin-33-deficient (IL-33 KO) mice,[6] IL-25 KO mice,[17] and TSLPR KO mice[18] were generated as previously reported. BALB/c wild-type mice purchased from Japan SLC (Shizuoka, Japan) and KO mice were backcrossed with them for at least seven generations to establish congenic IL-33 KO, IL-25 KO, and TSLPR KO mice. All animal experiments conformed to the Association for Research in Vision and Ophthalmology Statement on the Use of Animals in Ophthalmic and Vision Research.

Alum-RW Experimental Allergic Conjunctivitis

Mouse EAC was induced as previously described,[10] with slight modifications. Briefly, short RW pollen (Polysciences, Warrington, PA, USA) was emulsified using Imject Alum adjuvant (Thermo Scientific, Rockford, IL, USA). At day 0, 50 μL emulsified RW (50 μg RW with 50 μL alum) was injected into the left hind footpad and tail base, and serum was collected from the tail vein. Two weeks later, a second immunization was carried out using the right hind footpad. From days 26 to 29, the eyes of immunized mice were challenged daily with RW in phosphate-buffered saline (PBS) (2 mg in 10 μL per eye) or with PBS alone. Twenty minutes after the last eye-drop challenge, the EAC was evaluated using the scores for chemosis, redness, lid edema, tearing, discharge, and scratching behavior based on criteria described by Magone et al.[19] (Supplementary Table S1). At 24 hours after the last eye-drop challenge, the eyeballs (with lids and conjunctival tissue) were collected for histological analyses and quantification of cytokine expression. For IL-33 protein expression analysis, we made an ex vivo culture model of resected conjunctivae from eyes challenged with RW eye drops only once at day 26. Blood samples were also collected for the measurement of serum immunoglobulin E (IgE) levels at day 30.

Measurement of Serum IgE Levels

Total IgE levels in sera at days 0 and 30 were quantified using mouse IgE ELISA kits (ELISA MAX; Biolegend, San Diego, CA, USA), according to the manufacturer's protocol.

Histological Analysis

Eyeballs (with conjunctival tissues and eye lids) were dissected and fixed in 4% paraformaldehyde in PBS. Vertical 2-μ-thick paraffin sections were made and stained with Giemsa stain (Merk, Darmstadt, Germany). Throughout each section, infiltrating eosinophils in the lamina propria mucosae of the tarsal and bulbar conjunctivae were counted in the central portion of the eye, which included the pupil and optic nerve head, as described previously.[20]

Real-Time PCR Analysis

Conjunctival tissue obtained from the mouse eye was immediately submerged in RNA Later solution (Ambion, Austin, TX, USA) to protect the RNA. Total RNA was extracted from the tissue using an RNA isolation kit (NucleoSpin II; Macherey-Nagel GmbH, Duren, Germany). Complementary DNAs (cDNAs) were prepared using random primers and ReverTra Ace reverse transcriptase (both from Toyobo, Osaka, Japan), according to the manufacturer's protocol. Real-time PCR primers specific for mouse *il4*, *il5*, *il13*, *il33*, *ccl5*, *ccl11*, and *gapdh* mRNAs were designed by QuantPrime (Universitat Potsdam, Potsdam, Germany) and are summarized in Supplementary Table S2. Real-time PCR analysis was performed using a PRISM model 7300 HT (Applied Biosystems, Grand Island, NY, USA) sequence detection system with Fast SYBR green master mix (Life Technologies Japan, Tokyo, Japan). The relative expression levels of *il4*, *il5*, *il13*, *il33*, *ccl5*, and *ccl11* were quantified by comparative cycle threshold (C_t) methods using *gapdh* mRNA expression in the same cDNA as the internal controls.

Immunohistochemistry

Immunofluorescent staining was performed to examine IL-33 expression in the conjunctival tissue obtained from experimental conjunctivitis. A goat anti-mouse IL-33 polyclonal antibody was purchased from R&D Systems (Minneapolis, MN, USA), a rat anti-mouse F4/80 antibody (clone CI:A3-1; BioLegends), and a sheep anti-mouse mast cell protease (mcp) 1 antibody (clone MS-RM8; Moredun Scientific, Midlothian, UK). A basophil-specific rat anti-mouse mcp8 antibody was obtained from BioLegends,[21] and a rat anti-mouse major basic protein (MBP) antibody was provided by J. Lee (Mayo Clinic, Rochester, MN, USA).[22] Frozen sections (5 μm) were cut and then immunostained with the anti-IL-33, anti-MBP, anti-F4/80, and anti-mcp1 antibodies. Anti-mcp8 immunohistochemical staining was carried out using 2-μm paraffin sections. Stained slides were observed using confocal laser scanning microscopy (FV-1000; Olympus Corp., Tokyo, Japan). Negative control specimens were immunostained with control goat IgG or rat IgG antibodies (all from Santa Cruz Biotechnology, Santa Cruz, Dallas, TX, USA) instead of the primary antibodies. Double-immunostaining was carried out using goat anti-IL-33 antibody with the rat anti-MBP antibody, the rat anti-F4/80 antibody, or the sheep anti-mcp1 antibody. A donkey-Alexa 488-conjugated anti-rat IgG antibody, donkey-Alexa 594-conjugated anti-goat IgG antibody, and donkey-Alexa 488-conjugated anti-sheep IgG antibody (all from Life Technologies Japan) were used as secondary antibodies.

Measurement of IL-33 Protein Concentration in Supernatant of Ex Vivo Conjunctival Tissue Culture

At the indicated times (1, 3, 6, and 12 hours) after the RW eye-drop challenge, the mice were killed, and conjunctival tissues were sampled. Tissues were cultured in 1.5-mL sterile micro-centrifuge tubes (Eppendorf Japan, Tokyo, Japan) for 60 minutes, using 200 μL of serum-free culture medium (OPTI-MEM; Life Technologies Japan) with protease inhibitors (Complete Mini; Roche Diagnostics GmbH, Mannheim, Ger-

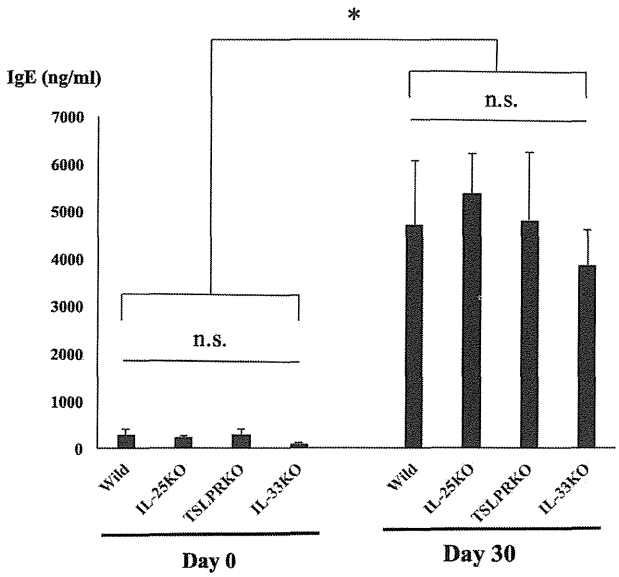

FIGURE 1. Total serum IgE measurement before and after RW-immunization. Total serum IgE concentration was quantified using ELISA at day 0 (before RW immunization) and on day 30 (after RW eye-drop challenges). A statistically significant increase (*$P < 0.01$, by Mann-Whitney U test) in IgE concentration was observed in day 0 samples compared to that in day 30 samples obtained from the same types of mice. There were no significant differences between day 0 and day 30 samples from the same types of mice (n.s., no significant differences). Data are triplicate measurements using five mice per each group and show mean ± SD IgE concentrations (ng/mL).

many). The IL-33 concentration in the supernatant of ex vivo tissue culture was quantified using mouse IL-33 Ready-SET-GO ELISA (eBioscience, San Diego, CA, USA) according to the manufacturer's protocol.

Statistical Analysis

Statistical evaluations of cell numbers, cytokine expression, serum IgE levels, and histological analysis were performed with the two-tail unpaired Mann-Whitney U test. A P value of <0.05 was considered statistically significant. All experiments were repeated at least three times, and representative data are shown.

RESULTS

Sera IgE Concentrations in RW-EAC Models

To evaluate the effect of RW sensitization and roles of type 2-initiating cytokines during the sensitization process, we measured sera IgE levels at day 0 (before sensitization) and at day 30 (after eye-drop challenge) by ELISA. Significant increases ($P < 0.01$) of total sera IgE at day 30 were observed in all types of mice (wild-type, IL-25 KO, IL-33 KO, and TSLPR KO) compared to those from day 0 samples of the same type of mice. There were no significant differences within day 0 samples and day 30 samples among the types of mice (Fig. 1).

Attenuated Clinical Symptoms of RW-Induced EAC in IL-33 KO Mice But Not in IL-25 KO or TSLPR KO Mice

Mice were immunized with RW in alum at days 0 and 14 and challenged from day 26, using RW or PBS eye drops daily for 4 days. Twenty minutes after the last challenge, we photographed and scored the severity of EAC by measuring the degree of chemosis, conjunctival redness, lid edema, tearing, discharge, and scratching, as shown in Supplementary Table S1. The clinical score for IL-33KO mice was significantly lower ($P = 0.011$) than that for wild-type mice (Figs. 2A, 2B, $n = 5$ per group). There were no significant differences among clinical scores for IL-25 KO, TSLPR KO, and wild-type mice (Fig. 2B).

IL-33 Deletion Diminished the Number of Eosinophils Infiltrating Conjunctivae of RW-Induced EAC

Twenty-four hours after the last RW eye-drop challenge, the eyes were collected, and the number of eosinophils was counted using Giemsa-stained slides (Fig. 3A). The number of eosinophils infiltrating the conjunctivae of IL-33 KO mice was significantly lower ($P = 0.011$) than those in wild-type mice (Fig. 3B, $n = 5$ per group). There were no significant

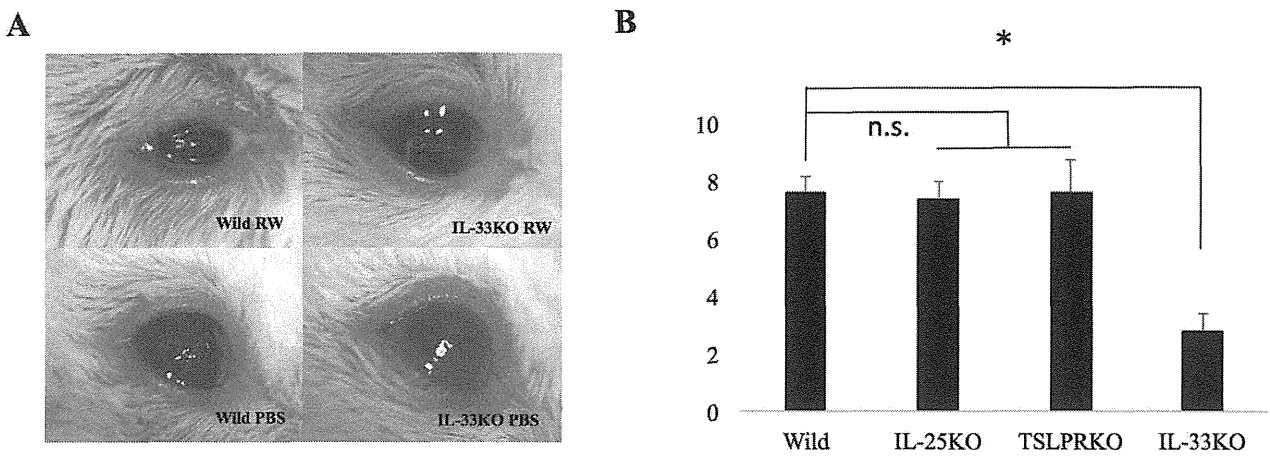

FIGURE 2. Clinical evaluation of RW-EAC. Representative photographs show RW-EAC models using wild-type and IL-33 KO mice challenged with either RW-PBS (*upper row*) or PBS alone (*lower row*), taken 20 minutes after the last eye-drop challenge (**A**). Clinical scores of the RW-challenged EAC models are shown (**B**). Data are representative mean ± SD clinical scores of five mice for each group (*$P < 0.05$, Mann-Whitney U test).

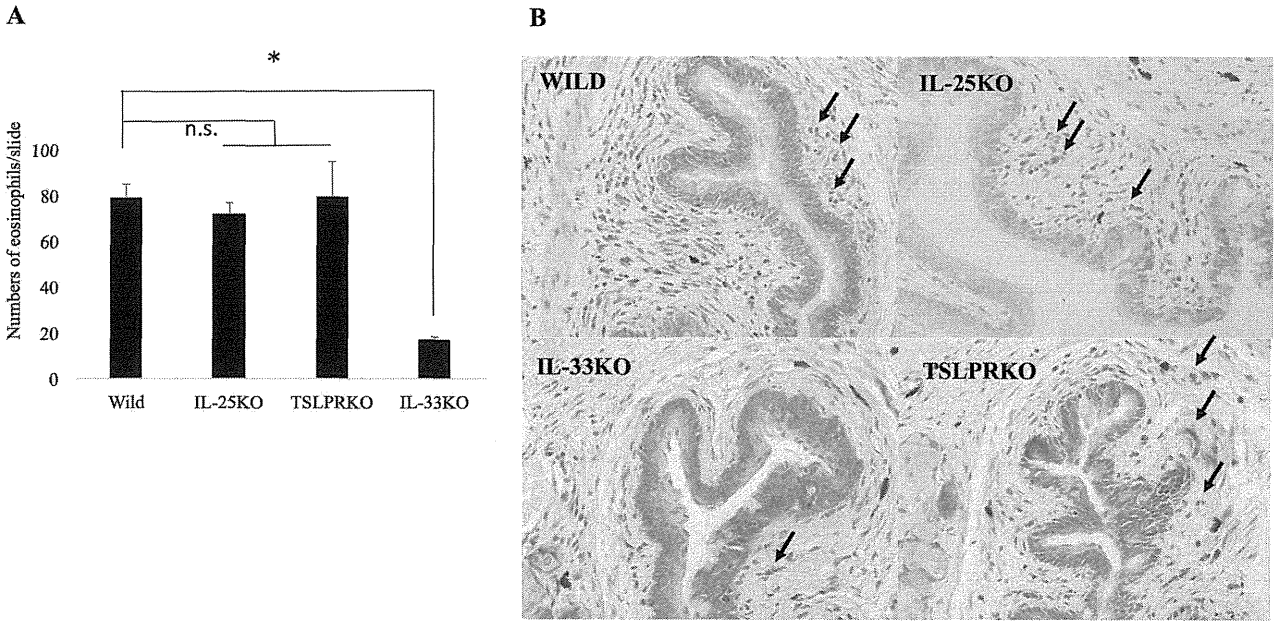

FIGURE 3. Eosinophil infiltration in conjunctivae of RW-EAC mice. Eyes of RW-EAC models were sampled 24 hours after the last RW challenge, and the numbers of eosinophils (*arrows*) infiltrating the substantia propria of the conjunctival tissues were counted using Giemsa-stained slides (**A**). Data are representative mean ± SD numbers of infiltrating eosinophils per slide counted in conjunctivae of five mice per group (**B**) (*$P < 0.05$, Mann-Whitney U test).

differences among the numbers of infiltrating eosinophils for IL-25 KO, TSLPR KO, and wild-type mice (Fig. 3B).

Quantification of Cytokine Expression in Mouse Conjunctival Tissues Obtained From RW-EAC Models

Conjunctival tissues were sampled 24 hours after the last RW eye-drop challenge, and their cytokine expression levels were quantified. Significant upregulation of *il4*, *il5*, *il13*, and *ccl5* mRNA expression ($P < 0.05$) was observed in the conjunctival tissue of RW-induced EAC in wild-type mice compared to that in PBS-challenged conjunctival tissue of wild-type mice (Fig. 4, asterisks). No significant upregulation of *ccl11* mRNA was induced by the RW eye-drop challenge. Significant attenuation of *il4*, *il5*, *il13*, and *ccl5* mRNA expression ($P < 0.01$) was observed in the IL-33 KO mice compared to that in wild-type mice (Fig. 4, double asterisks).

Time Courses of *il33* mRNA and IL-33 Protein Expression in RW-EAC Models

The IL-33 protein level in the ex vivo culture supernatant was significantly upregulated ($P < 0.05$) in the conjunctival tissue samples obtained at 1, 3, 6, and 12 hours after the first RW eye-drop challenge (Fig. 5A). No IL-33 protein was detected in the conjunctival tissue obtained from RW eye-drop-challenged IL-33 KO mice (data not shown). Significant *il33* mRNA upregulation ($P < 0.05$) was observed in the conjunctival tissue obtained from wild-type mice 1 hour after the last RW eye-drop challenge compared to that in PBS-challenged control tissue (Fig. 5B).

Immunohistochemical Analysis of EAC

Immunofluorescent staining was performed to examine the expression of IL-33 and the immunolocalization of eosinophils, macrophages, mast cells, and basophils in the conjunctival tissue obtained from EAC mice. Anti-mcp8 (basophil marker) immunostaining of the RW-EAC models showed basophil infiltration in the subepithelial regions of the RW-challenged eyes (Figs. 6A, 6B), and the number of infiltrating basophils was significantly higher (*$P < 0.05$) in the RW-EAC models of the wild-type mice than in IL-33 KO mice (Fig. 6E).

Ragweed-challenged conjunctivae of wild-type mice showed IL-33 protein expression in conjunctival epithelial cells and infiltrating cells of the substantia propria of the conjunctival tissue in the vicinity of MBP-positive eosinophils (Figs. 7B, 7C, arrowheads). Phosphate-buffered saline–challenged conjunctival tissue of wild-type mice showed IL-33-positive immunoreactivity in the epithelial cell layer (Fig. 7E, asterisk) and sparse infiltration of eosinophils in the subepithelial region (Fig. 7D). Conjunctival tissue of the RW-EAC model using IL-33KO mice had less MBP-positive eosinophil infiltration than in wild-type mice (Fig. 7G) and no IL-33-positive immunostaining was observed (Fig. 7H). Double immunohistochemical staining using the anti-IL-33 antibody and macrophage marker F4/80 antibody showed that some of the IL-33–positive cells in the substantia propria were also positive for F4/80 antigen (Figs. 8A–C, arrows). Similarly, some of the IL-33–positive cells in the substantia propria were also positive for the mast cell marker (mcp1) (Figs. 8D–F, arrowheads).

Discussion

To explore the roles of type 2–initiating cytokines (IL-25, IL-33, and TSLP) in the pathophysiology of allergic conjunctivitis, we made RW-EAC models by using IL-25 KO, IL-33 KO, and TSLPR KO mice. We first conducted preliminary studies to determine the intensity of allergic inflammation by changing the numbers of RW eye-drop challenges. We found that four RW eye-drop challenges produced appropriate and reproducible inflammation for further analysis. Measurement of serum total IgE showed clear upregulation of serum IgE in the RW-EAC models

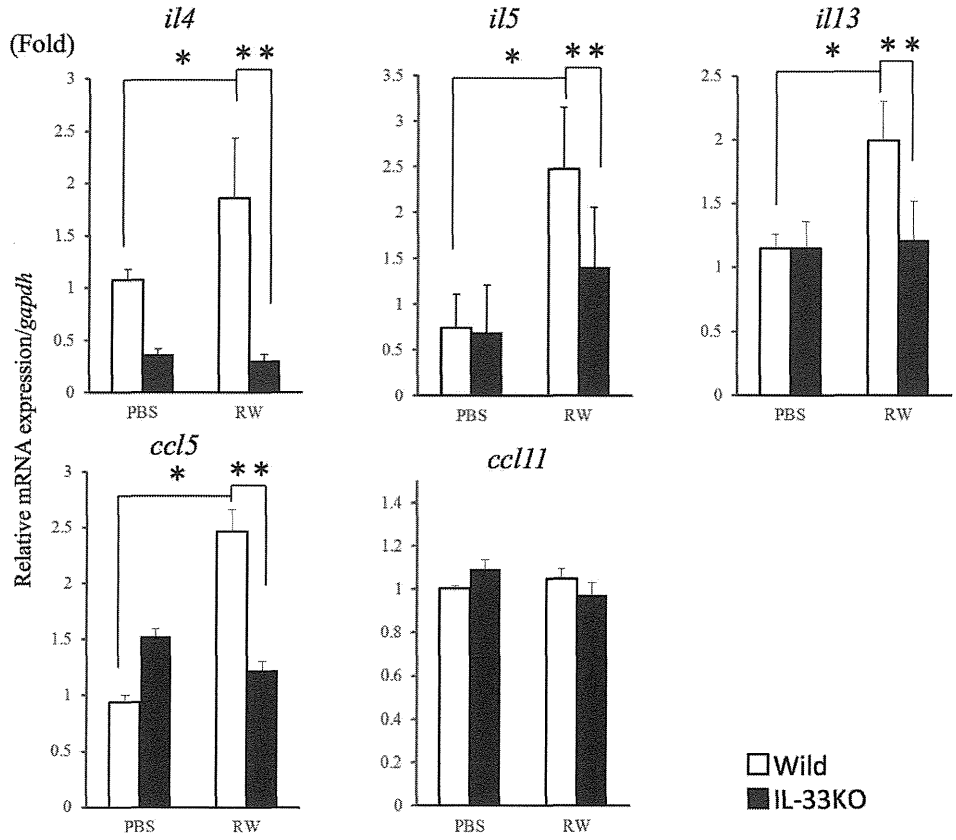

FIGURE 4. Quantification of cytokine mRNA expression in conjunctivae of RW-EAC models. Expression levels of inflammatory cytokine/chemokine (*il4*, *il5*, *il13*, *ccl5*, *ccl11*) mRNAs were quantified by real-time PCR. Relative mRNA expression is shown as fold changes of mRNA expression levels of PBS-challenged conjunctival tissues. Expression data were normalized to that of *gapdh* mRNA of the same cDNA samples. Significantly elevated expression levels of *il4*, *il5*, *il13*, and *ccl5* mRNAs were observed in RW-challenged conjunctivae of wild-type mice compared to those in PBS-challenged conjunctivae (*$P < 0.05$). Attenuated expression of *il4*, *il5*, *il13*, and *ccl5* mRNAs was observed in RW-challenged conjunctivae of IL-33 KO mice compared that in conjunctivae of wild-type mice (**$P < 0.05$). No differential *ccl11* mRNA expression levels were observed. Data are representative mean ± SD fold expression values of triplicate measurements.

(Fig. 1). The increase in serum IgE in our RW-EAC model was consistent with a previous report showing upregulation of serum IgE in an RW-EAC model[10] and in an RW-induced rhinitis model using BALB/c mice.[23] Nakinishi et al.[24] and Chu et al.[25] showed that there were no differences in increases of total serum IgE among IL-33 KO, IL-25 KO, TSLPR KO, and wild-type mice in an HDM-induced rhinitis model. Consistent with those reports, our results did not show significant differences in total sera IgE concentrations among the mouse types in the RW-EAC model (Fig. 1). On the other hand, Canbaz et al.[26] made an HDM-induced mouse airway inflammation model and showed that the total serum IgE level was IL-33 dependent in the case of HDM extracts with low endotoxin levels, whereas the IgE level was IL-33 independent in case of an HDM extract with high endotoxin levels. We consider that the type 2–initiating cytokines did not affect the IgE responses in our RW-EAC models, although the effect of IL-33 on IgE production was dependent on the model systems and the antigens used in the experiments.

Next, we compared clinical scores (Fig. 2; Supplementary Table S1) and numbers of infiltrating eosinophils (Fig. 3) in the RW-EAC models. Results showed that IL-33 deletion attenuated the clinical severity and diminished the eosinophil infiltration in the conjunctivae of the RW-EAC model. The attenuation of inflammation of RW-EAC in IL-33 KO mice in both the early phase clinical scores and the delayed phase eosinophilic infiltration were consistent with a previous report showing the role of IL-33 during the antigen challenge phase in an RW-EAC model.[11]

We found no significant differences among wild-type, TSLPR KO, and IL-25 KO mice with regard to clinical severity and numbers of eosinophils infiltrating the conjunctivae of the RW-EAC models (Figs. 2, 3). Results of inflammatory cytokine quantification showed attenuated *il5* mRNA expression but no differential expression of *il4*, *ccl5*, or *ccl11* mRNAs in the conjunctival tissues of the RW-EAC models using TSLPR-KO mice/IL-25 KO mice compared to those in wild-type mice (Supplementary Figs. S1, S2). Schleimer et al.[27] reported the effects of IL-5, CCL5, and CCL11 on the transendothelial migration of eosinophils. According to their results, IL-5 itself had a minimal effect on eosinophil migration but synergistic effects with CCL5 or with CCL11. The absence of differential expression of *ccl5* and *ccl11* mRNAs may account for the lack of a difference in eosinophil infiltration among TSLPR KO, IL-25 KO, and wild-type mice.

To further clarify the role of IL-33 in the pathophysiology of RW-EAC, chronological changes in IL-33 expression in the conjunctival tissue were examined. To quantify the IL-33 protein expression on the ocular surface in the RW-EAC model, we tried to detect IL-33 protein by simply collecting ocular surface exudate, using a small amount of PBS. However, the IL-33 concentration in the exudate was below

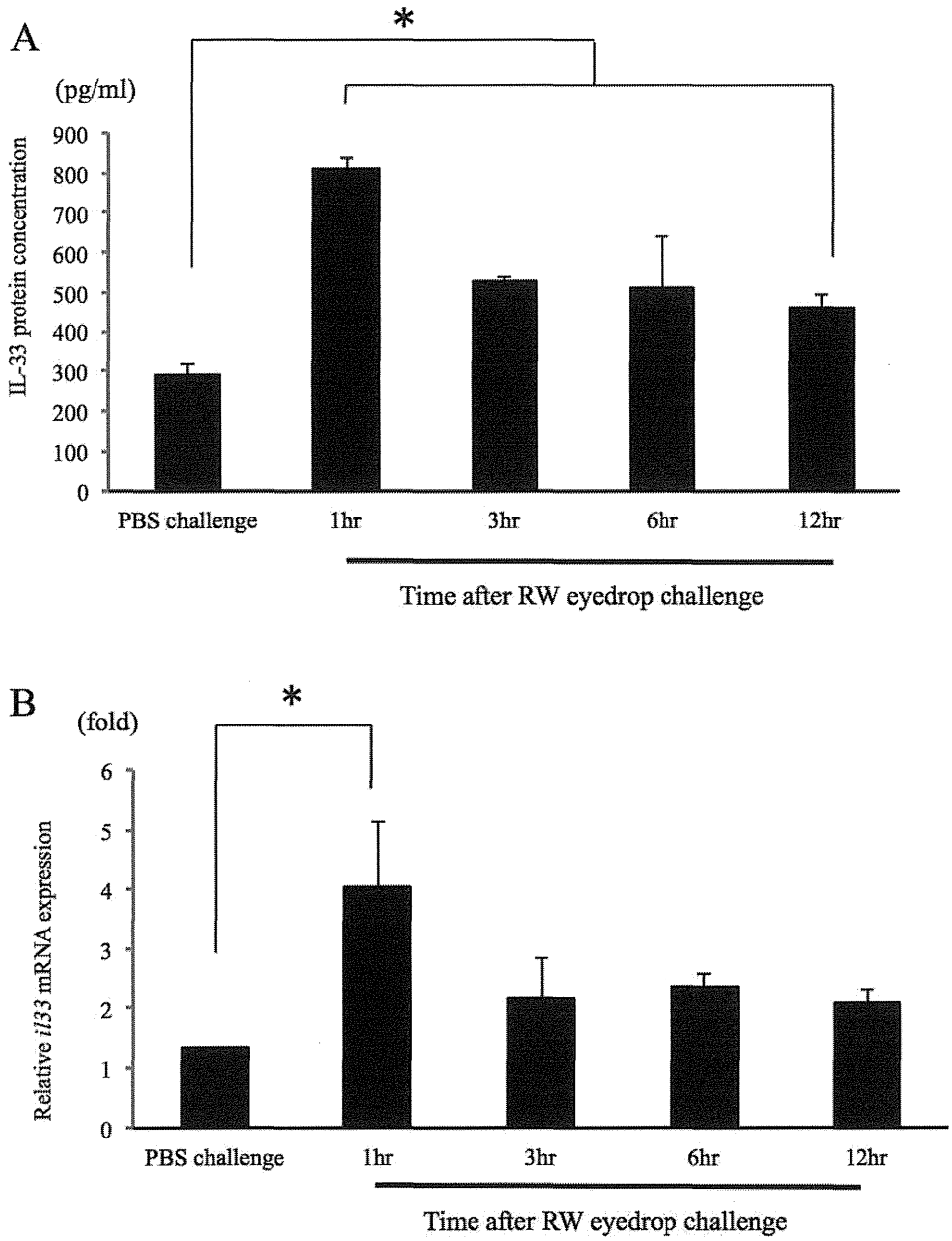

FIGURE 5. Time courses of IL-33 expression in the conjunctivae of RW-EAC models. Expression levels of IL-33 protein (**A**) and *il33* mRNA (**B**) at various time points (1, 3, 6, and 12 hours) after a single RW eye-drop challenge were quantified by ELISA and real-time PCR analysis, respectively. Interleukin-33 concentrations in culture supernatants of ex vivo–cultured conjunctivae tissues were quantified. Data are representative mean ± SD fold expression values using three conjunctivae for each time point, measured in duplicate. Significant upregulation was observed from 1 through 12 hours after eye-drop challenge (**A**). Relative mRNA expression is shown as fold change of mRNA expression levels in PBS-challenged conjunctival tissues. Data were normalized to the expression of *gapdh* mRNA of the same cDNA samples. Data are representative mean ± SD fold expression values of triplicate measurements. Significant upregulation was observed at 1 hour after eye-drop challenge but not at 3 to 12 hours (**B**) (*$P < 0.05$, Mann-Whitney U test).

the detection level (data not shown). Therefore, we measured the IL-33 protein concentrations in the ex vivo culture supernatant of conjunctival tissues obtained after RW challenge. A significant increase in IL-33 protein in the culture supernatants from 1, 3, 6, and 12 hours after RW eye-drop challenge peaked at 1 hour (Fig. 5A) suggested continuous IL-33 protein release from IL-33–producing cells. This rapid upregulation of IL-33 protein was consistent with the results from an RW-induced experimental rhinitis model in which IL-33 protein release was observed upon RW stimulation of nasal epithelium accompanied by temporal loss of IL-33 immunostaining.[23] Rapid release (1 hour after allergen challenge) of IL-33 protein was also observed in a model of lung inflammation induced by a mixture of allergens (HDM and *Aspergillus* and *Alternaria* spp.).[28] Transient upregulation of *il33* mRNA expression was observed at 1 hour after the RW eye-drop challenge (Fig. 5B). These results suggested that a rapid phase of IL-33 protein upregulation was

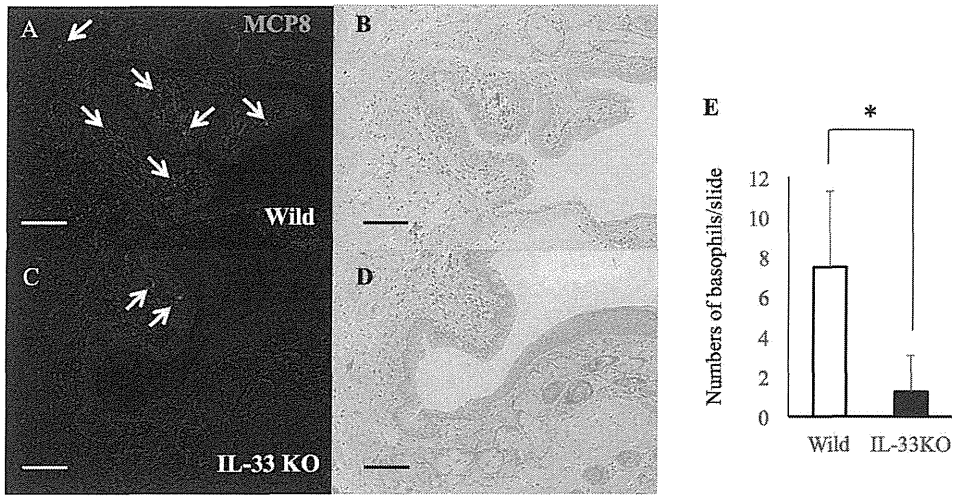

FIGURE 6. Mast cell protease 8–positive basophils in the conjunctivae of RW-EAC models. Mast cell protease 8 immunohistochemical staining of the conjunctiva showed higher numbers of mcp8-positive basophils (*arrows*) in the subepithelial regions of the RW-EAC model in wild-type mice (**A**) than in those of IL-33 KO mice (**C**). Hematoxylin and eosin staining of adjacent slides (**B**, **D**) is also shown. *Scale bars*: 100 μm. Mean ± SD numbers of basophils per slide in the conjunctivae of eight mice from each group are shown (**E**) (*$P < 0.05$, Mann-Whitney U test).

induced by the release of stored IL-33 from conjunctivae and that de novo IL-33 production might contribute later to continuous IL-33 release from conjunctivae.

We observed significant attenuation of *il4* mRNA expression in the conjunctivae of the RW-EAC model using IL-33 KO mice compared to that in wild-type mice (Fig. 4). Interleukin-4 is a key cytokine for type 2 immune responses mediated by adaptive immunity. It stimulates Th2 cell differentiation from naïve T cells and induces IL-5 and IL-13 expression.[29] The effects of IL-33 deletion on *il4* mRNA expression were significant even for eyes with mock eye-drop challenges, but it became more apparent with RW eye-drop challenge (Fig. 4). We observed diminished numbers of infiltrating basophils, which are known to produce a large amount of IL-4,[30] in the

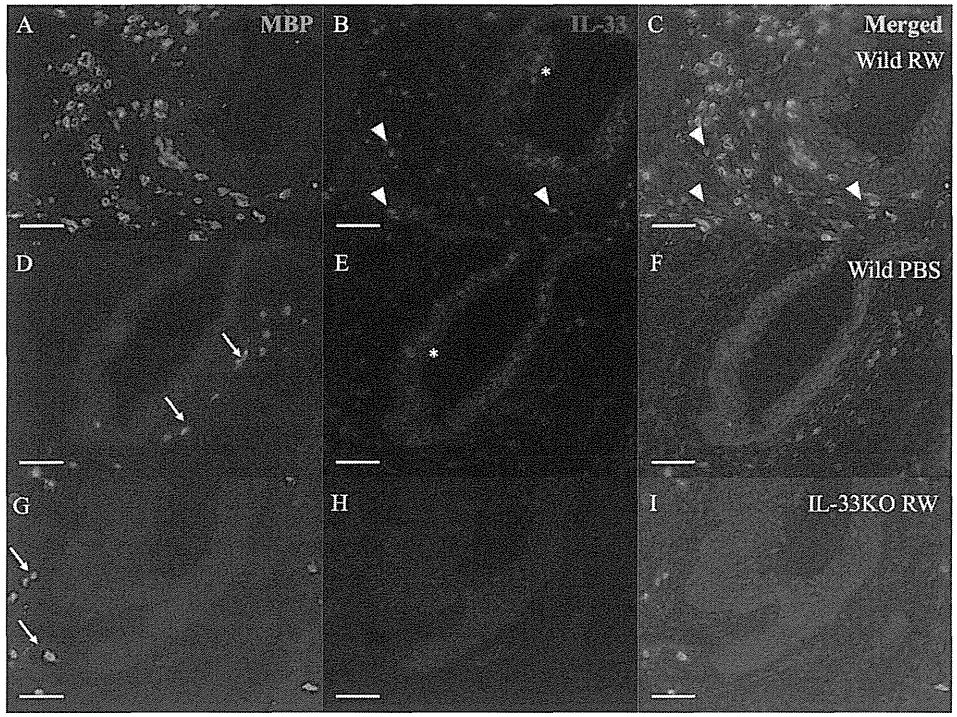

FIGURE 7. Interleukin-33 expression of in the conjunctivae of RW-EAC models. Anti-MBP (**A**, **D**, **G**) and anti-IL-33 (**B**, **E**, **H**) immunostaining of conjunctivae obtained from RW-EAC models are shown. Massive infiltration of MBP-positive eosinophils (*green*) is observed in substantia propria of RW-challenged EAC in wild-type mice (**A**). On the other hand, sparse infiltration of eosinophils was observed in PBS-challenged wild-type mice (**D**, **F**) and RW-challenged IL-33 KO mice (**G**). Interleukin-33 protein expression (*asterisks*) can be observed in the conjunctival epithelial cells of wild-type mice. Infiltrating cells of substantia propria in the vicinity of MBP-positive eosinophils (*arrowheads*) are also immunopositive for IL-33 (**B**, **C**). No IL-33–positive cells are observed in the conjunctivae of IL-33 KO mice (**H**, **I**). *Scale bars*: 50 μm.

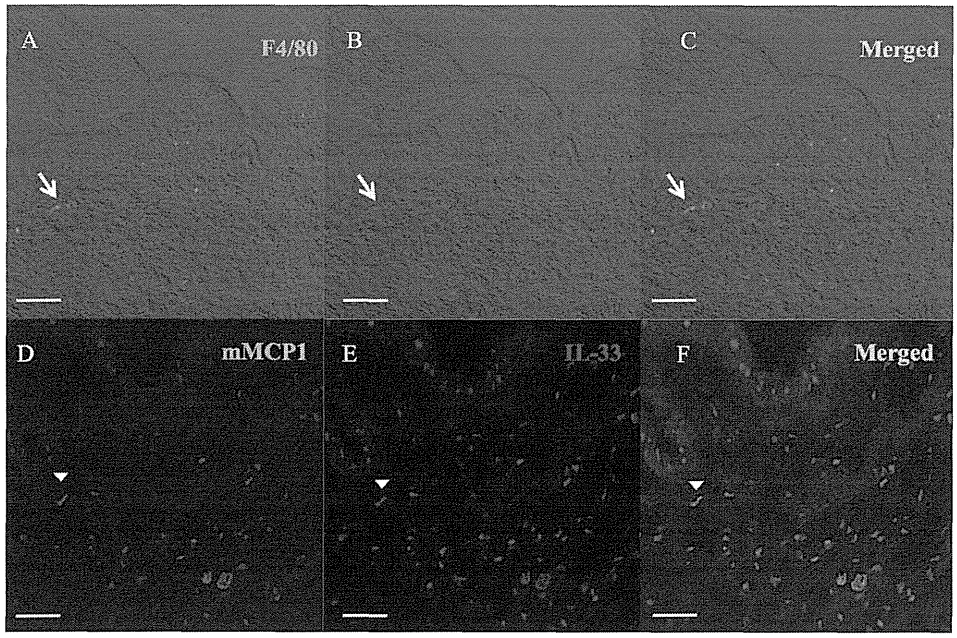

FIGURE 8. Colocalization of F4/80 and IL-33, as well as mMCP1 and IL-33, in substantia propria of the RW-EAC model. Some of the IL-33–positive cells (**B**, **E**) in substantia propria are also immunopositive for F4/80 ([**A**, **C**] *arrows*) or mMCP1 ([**D**, **F**] *arrowheads*). *Scale bars*: 50 μm.

conjunctivae of the RW-EAC model using IL-33 KO mice compared to the wild-type mice (Fig. 6). These results suggested that IL-33 might augment the expression of IL-4 in the RW-EAC model by promoting systemic basophil expansion or basophil infiltration into the EAC tissue. Our hypothesis is further supported by a report showing that IL-33 induces murine basophil expansion,[31] and another showing diminished numbers of basophils in the nasal tissue of an RW-induced rhinitis model using IL-33 KO mice.[23] We also found diminished *il4*, *il5*, and *il13* mRNA expression in cervical lymph node cells obtained from RW-EAC model IL-33 KO mice compared to those of the wild-type mice after in vitro stimulation using an RW extract for 48 hours (Supplementary Fig. S3). This result was consistent with a previous report on RW-induced rhinitis models using IL-33 KO,[23] and indicated diminished expression of cervical lymph node T cells in the IL-33 KO mice to produce Th2 cytokines.

The differential upregulation of *ccl5* (encoding the regulated on activation, normal T cell expressed and secreted [RANTES] protein) mRNA but not of *ccl11* (encoding eotaxin) mRNA, in the RW-EAC model in IL-33 KO mice suggested that IL-33 could induce *ccl5* expression (Fig. 4). These results were consistent with those in a report showing that IL-33 stimulation upregulated CCL5 protein expression but had only marginal effects on CCL11 expression in mast cells and in basophils.[23] In the RW-EAC model, we observed infiltration of basophils (Fig. 6) and mast cells (Fig. 8) in the conjunctival tissue; therefore IL-33 activated mast cells and basophils may play some roles in eosinophil infiltration in the RW-EAC model through the effect of CCL5, a well-known eosinophil chemoattractant.[32]

Immunohistochemical staining was positive for IL-33 not only in the cell nuclei of the conjunctival epithelium (as shown in previous reports[11,23]), but also in the infiltrating cells located in the substantia propria (Fig. 7). Figure 8 shows that some of the IL-33–positive cells were double-positive with a macrophage marker (F4/80) and mast cell marker (mMCP1). These results were consistent with previous reports showing that IL-33 is produced by mast cells[33] and activated macrophages.[34] Considering these results together, we concluded that not only epithelial cells but also macrophages and mast cells were the source of IL-33 in RW-EAC models.

It should also be noted that there was no apparent IL-33 positive staining in the vascular endothelia of conjunctival tissues obtained from the RW-EAC models (Fig. 7), whereas in human conjunctival tissues obtained from AKC/VKC patients, the vascular endothelium (especially high endothelial venules) is immunopositive for IL-33.[4] The limitations of the present study are the feasibility of RW-induced allergic conjunctivitis as a model for severe human chronic allergic conjunctivitis in which exposure to multiple, and divergent allergens (e.g., HDM, pollen, and animal-derived antigens) cause severe chronic allergic conjunctivitis, and the differences of IL-33 expression between human and mouse tissues, especially in the vascular endothelium.

In conclusion, among the epithelial cell–derived type 2–initiating cytokines, we demonstrated the indispensable role of IL-33 in the pathophysiology of RW-EAC. Targeting IL-33 signaling cascades on the ocular surface using a decoy receptor (soluble ST2) for IL-33 might be a promising therapeutic method for ocular allergic diseases.

Acknowledgments

Supported by Grants-in-Aid 24659768 and 26462698 from the Japanese Society for the Promotion of Science and by the Takeda Science Foundation.

Disclosure: **Y. Asada**, None; **S. Nakae**, None; **W. Ishida**, None; **K. Hori**, None; **J. Sugita**, None; **K. Sudo**, None; **K. Fukuda**, None; **A. Fukushima**, None; **H. Suto**, None; **A. Murakami**, None; **H. Saito**, None; **N. Ebihara**, None; **A. Matsuda**, None

References

1. Pulendran B, Artis D. New paradigms in type 2 immunity. *Science*. 2012;337:431–435.
2. Galli SJ, Tsai M, Piliponsky AM. The development of allergic inflammation. *Nature*. 2008;454:445–454.

3. Oliphant CJ, Barlow JL, McKenzie AN. Insights into the initiation of type 2 immune responses. *Immunology.* 2011; 134:378–385.
4. Matsuda A, Okayama Y, Terai N, et al. The role of interleukin-33 in chronic allergic conjunctivitis. *Invest Ophthalmol Vis Sci.* 2009;50:4646–4652.
5. Matsuda A, Ebihara N, Yokoi N, et al. Functional role of thymic stromal lymphopoietin in chronic allergic keratoconjunctivitis. *Invest Ophthalmol Vis Sci.* 2010;51:151–155.
6. Oboki K, Ohno T, Kajiwara N, et al. IL-33 is a crucial amplifier of innate rather than acquired immunity. *Proc Natl Acad Sci U S A.* 2010;107:18581–18586.
7. Stolarski B, Kurowska-Stolarska M, Kewin P, Xu D, Liew FY. IL-33 exacerbates eosinophil-mediated airway inflammation. *J Immunol.* 2010;185:3472–3480.
8. Eiwegger T, Akdis CA. IL-33 links tissue cells, dendritic cells and Th2 cell development in a mouse model of asthma. *Eur J Immunol.* 2011;41:1535–1538.
9. Morita H, Arae K, Ohno T, et al. ST2 requires Th2-, but not Th17-, type airway inflammation in epicutaneously antigen-sensitized mice. *Allergol Int.* 2012;61:265–273.
10. Fukushima A, Yamaguchi T, Ishida W, et al. Genetic background determines susceptibility to experimental immune-mediated blepharoconjunctivitis: comparison of Balb/c and C57BL/6 mice. *Exp Eye Res.* 2006;82:210–218.
11. Matsuba-Kitamura S, Yoshimoto T, Yasuda K, et al. Contribution of IL-33 to induction and augmentation of experimental allergic conjunctivitis. *Int Immunol.* 2010;22:479–489.
12. Takai T. TSLP expression: cellular sources, triggers, and regulatory mechanisms. *Allergol Int.* 2012;61:3–17.
13. Liu YJ, Soumelis V, Watanabe N, et al. TSLP: an epithelial cell cytokine that regulates T cell differentiation by conditioning dendritic cell maturation. *Annu Rev Immunol.* 2007;25:193–219.
14. Zheng X, Ma P, de Paiva CS, et al. TSLP and downstream molecules in experimental mouse allergic conjunctivitis. *Invest Ophthalmol Vis Sci.* 2010;51:3076–3082.
15. Fort MM, Cheung J, Yen D, et al. IL-25 induces IL-4, IL-5, and IL-13 and Th2-associated pathologies in vivo. *Immunity.* 2001; 15:985–995.
16. Angkasekwinai P, Park H, Wang YH, et al. Interleukin 25 promotes the initiation of proallergic type 2 responses. *J Exp Med.* 2007;204:1509–1517.
17. Ishii A, Oboki K, Nambu A, et al. Development of IL-17-mediated delayed-type hypersensitivity is not affected by down-regulation of IL-25 expression. *Allergol Int.* 2010;59: 399–408.
18. Carpino N, Thierfelder WE, Chang MS, et al. Absence of an essential role for thymic stromal lymphopoietin receptor in murine B-cell development. *Mol Cell Biol.* 2004;24:2584–2592.
19. Magone MT, Chan CC, Rizzo LV, Kozhich AT, Whitcup SM. A novel murine model of allergic conjunctivitis. *Clin Immunol Immunopathol.* 1998;87:75–84.
20. Ishida W, Fukuda K, Kajisako M, et al. B and T lymphocyte attenuator regulates the development of antigen-induced experimental conjunctivitis. *Graefes Arch Clin Exp Ophthalmol.* 2012;250:289–295.
21. Ugajin T, Kojima T, Mukai K, et al. Basophils preferentially express mouse Mast Cell Protease 11 among the mast cell tryptase family in contrast to mast cells. *J Leukoc Biol.* 2009; 86:1417–1425.
22. Larson KA, Horton MA, Madden BJ, Gleich GJ, Lee NA, Lee JJ. The identification and cloning of a murine major basic protein gene expressed in eosinophils. *J Immunol.* 1995;155:3002–3012.
23. Haenuki Y, Matsushita K, Futatsugi-Yumikura S, et al. A critical role of IL-33 in experimental allergic rhinitis. *J Allergy Clin Immunol.* 2012;130:184–194.
24. Nakanishi W, Yamaguchi S, Matsuda A, et al. IL-33, but not IL-25, is crucial for the development of house dust mite antigen-induced allergic rhinitis. *PLoS One.* 2013;8:e78099.
25. Chu DK, Llop-Guevara A, Walker TD, et al. IL-33, but not thymic stromal lymphopoietin or IL-25, is central to mite and peanut allergic sensitization. *J Allergy Clin Immunol.* 2013; 131:187–200.
26. Canbaz D, Utsch L, Logiantara A, van Ree R, van Rijt LS. IL-33 promotes the induction of immunoglobulin production after inhalation of house dust mite extract in mice. *Allergy.* 2015;70: 522–532.
27. Shahabuddin S, Ponath P, Schleimer RP. Migration of eosinophils across endothelial cell monolayers: interactions among IL-5, endothelial-activating cytokines, and C-C chemokines. *J Immunol.* 2000;164:3847–3854.
28. Iijima K, Kobayashi T, Hara K, et al. IL-33 and thymic stromal lymphopoietin mediate immune pathology in response to chronic airborne allergen exposure. *J Immunol.* 2014;193: 1549–1559.
29. Paul WE, Zhu J. How are T(H)2-type immune responses initiated and amplified? *Nat Rev Immunol.* 2010;10:225–235.
30. Karasuyama H, Mukai K, Obata K, Tsujimura Y, Wada T. Nonredundant roles of basophils in immunity. *Annu Rev Immunol.* 2011;29:45–69.
31. Schneider E, Petit-Bertron AF, Bricard R, et al. IL-33 activates unprimed murine basophils directly in vitro and induces their in vivo expansion indirectly by promoting hematopoietic growth factor production. *J Immunol.* 2009;183:3591–3597.
32. Schroder JM, Kameyoshi Y, Christophers E. RANTES, a novel eosinophil-chemotactic cytokine. *Ann N Y Acad Sci.* 1994; 725:91–103.
33. Hsu CL, Neilsen CV, Bryce PJ. IL-33 is produced by mast cells and regulates IgE-dependent inflammation. *PLoS One.* 2010;5: e11944.
34. Talabot-Ayer D, Calo N, Vigne S, Lamacchia C, Gabay C, Palmer G. The mouse interleukin (Il)33 gene is expressed in a cell type- and stimulus-dependent manner from two alternative promoters. *J Leukoc Biol.* 2012;91:119–125.

Jpn J Ophthalmol (2015) 59:216–222
DOI 10.1007/s10384-015-0388-y

THE OFFICIAL INTERNATIONAL JOURNAL OF THE JAPANESE OPHTHALMOLOGICAL SOCIETY

CLINICAL INVESTIGATION

Effects of corneal irregular astigmatism on visual acuity after conventional and femtosecond laser-assisted Descemet's stripping automated endothelial keratoplasty

Daisuke Tomida[1] · Takefumi Yamaguchi[1,2] · Akiko Ogawa[1,2] · Yumiko Hirayama[1] · Seika Shimazaki-Den[1] · Yoshiyuki Satake[1] · Jun Shimazaki[1,2]

Received: 19 December 2014 / Accepted: 10 April 2015 / Published online: 2 June 2015

Abstract

Purpose To compare short-term outcomes of Descemet's stripping automated endothelial keratoplasty (DSAEK) using a graft prepared with either a femtosecond laser or a microkeratome.

Methods Thirty-eight patients underwent DSAEK with grafts prepared with either a femtosecond laser (f-DSAEK; 21 eyes) or a microkeratome (m-DSAEK; 17 eyes). Visual acuity, endothelial cell density, regular astigmatism and irregular astigmatism were compared between the two groups preoperatively and at 1, 3, and 6 months post-operatively. Fourier analysis was conducted to calculate astigmatism of the anterior and posterior surfaces, and total cornea, using anterior segment optical coherence tomography (AS-OCT).

Results Visual acuity (logMAR) improved from 1.20 ± 0.60 to 0.43 ± 0.25 after m-DSAEK ($P < 0.001$) and from 1.20 ± 0.57 to 0.77 ± 0.33 after f-DSAEK ($P = 0.0028$) at 6 months following DSAEK. Visual acuity after m-DSAEK was significantly better than after f-DSAEK at 1, 3, and 6 months ($P < 0.05$). AS-OCT corneal images revealed greater irregularities on the posterior surfaces of f-DSAEK grafts compared to m-DSAEK grafts. Irregular astigmatism of the total cornea and the posterior surface was significantly larger after f-DSAEK than after m-DSAEK, although there was no significant difference in irregular astigmatism of the anterior surface at 6 months. Postoperative visual acuity was significantly correlated with the postoperative irregular astigmatism of the total cornea ($r = 0.6657$ and $P < 0.001$) and the anterior ($r = 0.416$, $P = 0.016$) and posterior surfaces ($r = 0.7046$, $P < 0.001$).

Conclusions Visual outcomes after f-DSAEK were poor compared to conventional m-DSAEK due to an increase in irregular astigmatism caused by posterior surface irregularities.

Keywords Endothelial keratoplasty · Femtosecond laser · Higher order aberration · Anterior segment imaging

Introduction

Descemet's stripping automated endothelial keratoplasty (DSAEK) has become a common surgical procedure for the treatment of endothelial dysfunction [1, 2]. Although DSAEK has several advantages over penetrating keratoplasty (PK), such as rapid visual recovery, less postoperative astigmatism, fewer higher-order aberrations (HOAs) and a decreased rejection rate [3–6], not all patients achieve greater visual acuity, despite the improved corneal clarity DSAEK provides. The reasons for poor visual acuity after DSAEK include HOAs and interface or subepithelial opacities [7–11]. In both a normal cornea and a post-PK cornea, the anterior and posterior surfaces of the cornea are parallel, which enables them to compensate for astigmatism and HOAs [12, 13]. After DSAEK, however, the posterior surface of the corneal graft disrupts this parallelism and increases HOAs of the total cornea by up to 25 % [13]. DSAEK graft asymmetry can cause optical degradation, which leads to poor visual function [14].

✉ Takefumi Yamaguchi
tym.i.eye.i@gmail.com

[1] Department of Ophthalmology, Ichikawa General Hospital, Tokyo Dental College, 5-11-13, Sugano, Ichikawa, Chiba 272-8513, Japan

[2] Department of Ophthalmology, Keio University School of Medicine, Tokyo, Japan

Preparation of a lamellar graft using a microkeratome is a widely known procedure but it has limitations, including limited ability to predict graft thickness and irregular graft geometry. Femtosecond laser (fs-laser) technology has been used to create flaps in situ (keratomileusis), arcuate incisions, and channels for intracorneal rings, and to prepare donor and host tissue for lamellar keratoplasty and PK [15–20]. Because the fs-laser can produce fine cuts and customize tissue geometry and size with high accuracy, fs-laser-assisted DSAEK (f-DSAEK) has been expected to provide better postoperative visual acuity. However, reports indicate that f-DSAEK visual outcomes are not favorable [21, 22], and the reasons for the poor visual outcomes are not clear. In this study, visual acuity, corneal regular astigmatism and irregular astigmatism were evaluated following f-DSAEK and compared to conventional DSAEK using a microkeratome (m-DSAEK) to identify the cause of poor visual outcome after f-DSAEK.

Subjects and methods

This study was approved by the university's clinical research ethics board and performed according to the Declaration of Helsinki.

Subjects

Thirty-eight patients that underwent DSAEK at the Tokyo Dental College Ichikawa General Hospital between April 2012 and July 2013 were included. In 21 consecutive DSAEK cases between February 2013 and July 2013, the donor corneas were prepared using a 150 kHz iFS fs-laser (Abbott Medical Optics, Santa Ana, CA, USA), whereas in 17 consecutive DSAEK cases between April 2012 and December 2012 the donor corneas were prepared using a microkeratome (M2, Moria, Antony, France). Details of the subjects are shown in Table 1. There were no statistical differences in any parameters between the preoperative groups. Some donor corneas were obtained from the Corneal Center Eye Bank of Tokyo Dental College and some from SightLife (Northwest Lions Foundation, http://www.sightlife.org/sightlife.cfm). All of the DSAEK grafts were precut and prepared in Tokyo Dental College Ichikawa General Hospital. During the study period, four eyes in the f-DSAEK group had primary graft failure and one eye in the m-DSAEK group developed neovascular glaucoma after DSAEK. Those five eyes were excluded from the analysis.

Donor cornea evaluation and preparation

All donor corneas were preserved in organ culture medium according to a standard protocol. Preoperative endothelial cell density (ECD) of the donor graft was evaluated with a specular microscope (EKA-10, Konan Kerato Analyzer, Hyogo, Japan). In both treatment groups, corneal grafts were prepared either the day before surgery or on the day of surgery. Corneas were mounted on a Moria artificial chamber. Physiological saline was used to maintain an anterior chamber with a bottle height of 80 cm. All grafts for m-DSAEK were prepared using a 350-μm M2 microkeratome (Moria, Antony, France). A single pass of the microkeratome was performed, averaging about 5 s per pass. The intended graft thickness was 150 μm. The grafts for f-DSAEK were prepared using the 150-kHz iFS fs-laser with the following settings: flap = 420 μm or less, raster energy = 1.4 μJ, spot sep/line sep = 7 μm/7 μm. The depth of lamellar cut by the fs-laser was set to produce a graft thickness of approximately 120 μm. Briefly, the cut depth was determined by subtracting 120 μm from the central corneal thickness of the donor graft. If the cornea thickness was more than 540 μm, the cut depth was set as

Table 1 Patient data

	f-DSAEK group	m-DSAEK group	*P* value
N	21	17	
Age (years)	70.0 ± 11.3	73.1 ± 5.0	0.29
Sex (Female/Male)	8/13	6/11	0.86
Preoperative			
CDVA (LogMAR)	1.20 ± 0.57	1.20 ± 0.60	0.94
Astigmatism (*D*)	2.75 ± 2.8	2.09 ± 1.41	0.41
Corneal thickness (μm)	749.8 ± 123.2	698.5 ± 104.7	0.19
Causative disease (*n*)			
Pseudophakic	4	3	0.91
After laser iridotomy	4	5	0.45
Fuchs' dystrophy	2	4	0.24
After trabeculectomy	3	0	0.10
Others	8	5	0.19

420 μm because 420 μm depth is the maximum possible in a safe and accurate cut of the cornea using the iFS fs-laser. The anterior lamellar cap was put on the cornea and returned into the corneal storage medium (Optisol GS, Bausch & lomb, Irvine, CA, USA) until the DSAEK surgery in both groups. All of the DSAEK were performed within 7 days from death to surgery.

Surgical procedures and follow-up

Following the injection of either retrobulbar or sub-Tenon's anesthesia (2 % lidocaine), DSAEK was performed through a 5.0-mm corneal or corneoscleral temporal incision. A 25-G infusion canula system was used to maintain the anterior chamber. In both groups, the size of the DSAEK graft was determined and the donor graft was trephinated using a Hessburg-Barron trephine, most commonly at an 8.0 mm diameter. Grafts were gently inserted into the anterior chamber with a Busin glide spatula using the double-glide technique [23]. The temporal incision was sutured with 10–0 nylon. Air was carefully injected into the anterior chamber to allow the graft to adhere. After 10 min, the air was reduced to about 50 % of the anterior chamber volume with BSS at the end of surgery. Patients were prescribed topical antibiotics (Levofloxacin, Cravit®, Santen Pharmaceutical Co., Osaka, Japan) and 0.1 % betamethasone (Sanbetazon®, Santen Pharmaceutical Co.) 5 times a day. These drops were tapered in the following months. Best corrected visual acuity (BCVA) and ECD were measured at 1, 3, and 6 months postoperation. Visual acuity was measured by using the standard Snellen chart and BCVA with correction was recorded. The results were converted into logarithm of minimal angle resolution (logMAR) units. ECD was measured using specular microscopy (SP-3000P, Topcon, Tokyo, Japan).

Anterior segment optical coherence tomography

Recipients' eyes were examined using anterior segment optical coherence tomography (AS-OCT, SS-1000, Tomey, Nagoya, Japan) preoperatively and 1, 3, and 6 months after the operation. All subjects were examined until at least two sets of excellent images were obtained. Sixteen rotating AS-OCT scans were taken to reconstruct a 3D model of the entire corneal configuration. The CASIA system corrected distortions in the AS-OCT images based on the refractive index of the anterior surface. Regular astigmatism and irregular astigmatism were calculated using the installed software [24]. The dioptric power of 256 concentric circles (0.019 mm interval within 9.8 mm diameter) on the anterior, posterior, and total corneal surface was transformed into trigonometric components up to the 14th order using Fourier analysis [24]. Regular astigmatism and irregular astigmatism were obtained from the Fourier analysis coefficients. Higher-order irregularity (HOI) was defined as the sum of the 3rd to 14th order coefficients.

Table 2 Pre- and postoperative visual acuity (logMAR)

	f-DSAEK	m-DSAEK	*P* value
Preop	1.20 ± 0.57	1.20 ± 0.60	0.94
1 month	0.80 ± 0.40	0.49 ± 0.24	0.01
3 months	0.72 ± 0.26	0.39 ± 0.23	0.001
6 months	0.77 ± 0.33	0.43 ± 0.25	0.001

Statistical analysis

Data were analyzed using statistical analysis software (SSRI Co. Ltd., Tokyo, Japan). The paired *t*-test was used to compare HOIs between the anterior, posterior, and total corneal surfaces in each treatment group. The Mann–Whitney *U* test was used to compare postoperative logMAR, ECD, and HOIs between the groups. Pearson's correlation analysis was used to evaluate the correlation between logMAR and HOIs of the anterior, posterior, and total corneal surface. A P-value less than 0.05 was considered statistically significant.

Results

Postoperative visual acuity

Visual acuity (logMAR) improved from 1.20 ± 0.57 to 0.43 ± 0.25 6 months after m-DSAEK ($P < 0.001$) and from 1.20 ± 0.60 to 0.77 ± 0.33 6 months after f-DSAEK ($P = 0.003$, Table 2). Comparing the postoperative visual acuity between m-DSAEK and f-DSAEK, postoperative visual acuity at 1, 3, and 6 months was significantly better after m-DSAEK than f-DSAEK at all time points ($P < 0.05$).

Postoperative complications

Graft dislocation occurred in 9 eyes out of 25 eyes after f-DSAEK (36 %) and in 3 eyes out of 18 eyes after m-DSAEK (17 %) ($P = 0.191$). Air injection was performed in all eyes with postoperative graft dislocation, however, in 3 f-DSAEK eyes, graft attachment was not obtained and graft suturing during the third air injection was required. Four patients in the f-DSAEK had primary graft failure, necessitating m-DSAEK.

Regular astigmatism and HOIs

Regular astigmatism characteristics and HOIs for both groups are shown in Tables 3 and 4. Figure 1 shows the

Table 3 Regular astigmatism of total cornea, anterior, and posterior surfaces

	f-DSAEK	m-DSAEK	*P* value
Total cornea			
Preop	1.00 ± 0.49	1.18 ± 0.79	0.24
1 month	1.81 ± 0.49	0.99 ± 0.68	0.02
3 months	1.25 ± 0.74	0.87 ± 0.61	0.07
6 months	1.17 ± 0.90	0.83 ± 0.49	0.11
Anterior surface			
Preop	0.96 ± 0.58	1.13 ± 0.82	0.27
1 month	1.75 ± 1.51	0.99 ± 0.66	0.04
3 months	1.26 ± 0.75	0.81 ± 0.61	0.04
6 months	1.19 ± 0.91	0.80 ± 0.47	0.08
Posterior surface			
Preop	0.34 ± 0.15	0.29 ± 0.16	0.19
1 month	0.38 ± 0.22	0.28 ± 0.20	0.10
3 months	0.29 ± 0.16	0.28 ± 0.23	0.40
6 months	0.26 ± 0.12	0.20 ± 0.06	0.05

Table 4 Higher-order irregularity of total cornea, anterior, and posterior surfaces

	f-DSAEK	m-DSAEK	*P* value
Total cornea			
Preop	0.75 ± 0.47	0.82 ± 0.80	0.39
1 month	0.71 ± 0.38	0.42 ± 0.19	0.005
3 months	0.52 ± 0.19	0.40 ± 0.14	0.03
6 months	0.45 ± 0.15	0.34 ± 0.12	0.02
Anterior surface			
Preop	0.69 ± 0.53	0.75 ± 0.83	0.40
1 month	0.69 ± 0.42	0.37 ± 0.14	0.005
3 months	0.45 ± 0.21	0.36 ± 0.13	0.09
6 months	0.39 ± 0.17	0.32 ± 0.13	0.14
Posterior surface			
Preop	0.27 ± 0.23	0.23 ± 0.16	0.33
1 month	0.35 ± 0.29	0.18 ± 0.11	0.02
3 months	0.27 ± 0.10	0.13 ± 0.08	<0.001
6 months	0.23 ± 0.11	0.11 ± 0.03	<0.001

representative cases after m-DSAEK and f-DSAEK. The regular astigmatism of the anterior surface at 1 and 3 months after f-DSAEK was significantly larger than after m-DSAEK ($P = 0.04$). However, there were no significant differences in the regular astigmatism of the posterior surface between f-DSAEK and m-DSAEK. The HOIs of the total cornea and posterior surface were significantly larger after f-DSAEK than after m-DSAEK during the entire 6-month follow-up period. The HOI of the anterior surface after f-DSAEK was significantly larger than after m-DSAEK at 1 month, but there were no significant differences at the 3- and 6-month follow-ups.

Endothelial cell density

Table 5 shows the time-course decrease of ECD after DSAEK. The graft ECDs were 2704 ± 677 cells/mm^2 and 2660 ± 285 cells/mm^2 for f-DSAEK and m-DSAEK, respectively. The postoperative ECD in eyes after f-DSAEK were 1220 ± 467 cells/mm^2 at 3 months and 1418 ± 530 cells/mm^2 at 6 months. The postoperative ECD in eyes after m-DSAEK were 1526 ± 489 cells/mm^2 at 3 months and 1514 ± 579 cells/mm^2 at 6 months. There were no significant differences in ECD between f-DSAEK and m-DSAEK.

Influence of HOIs on visual acuity

LogMAR was significantly correlated with the HOI of the total cornea and the HOIs of the anterior and posterior surfaces at 6 months post-DSAEK (Fig. 2, $r = 0.6657$, $P < 0.001$, $r = 0.413$, $P = 0.016$, and $r = 0.7046$, $P < 0.001$, respectively). The HOI of the total cornea was significantly correlated with the anterior and posterior surfaces ($r = 0.8424$, $P < 0.001$, and $r = 0.4494$, $P = 0.0164$, respectively), although the HOI of the anterior surface was not significantly correlated with the HOI of the posterior surface ($r = 0.117$, $P = 0.3664$).

Discussion

This study evaluated the influence of irregular astigmatism of the cornea on visual acuity after f-DSAEK and m-DSAEK. Our data demonstrate that an irregular graft causes irregular astigmatism of the posterior surface, which leads to irregular astigmatism of the total cornea after f-DSAEK. The irregular astigmatism after f-DSAEK results in poor visual outcome. It is documented that the fs-laser is safe and effective for DSAEK [1, 21, 25–27], but previous reports of f-DSAEK suggest that visual outcomes are inferior to m-DSAEK. Visual acuity after conventional m-DSAEK generally improves to 20/30 or better [28, 29]. However, in two studies the mean visual acuity after f-DSAEK is reported to be 20/87 [1] and 20/94 [22] at 6 months: lower than conventional PK. Vetter et al. report that the mean visual acuity after f-DSAEK was 0.48 logMAR and significantly worse than after m-DSAEK [27]. A report by Rosa et al. is unique in that DSAEK grafts were prepared using both an fs-laser and a microkeratome, and the postoperative visual acuity was excellent (0.11 logMAR) at 6 months [26]. Vetter et al. evaluated the irregularity of the posterior corneal surface after f-DSAEK

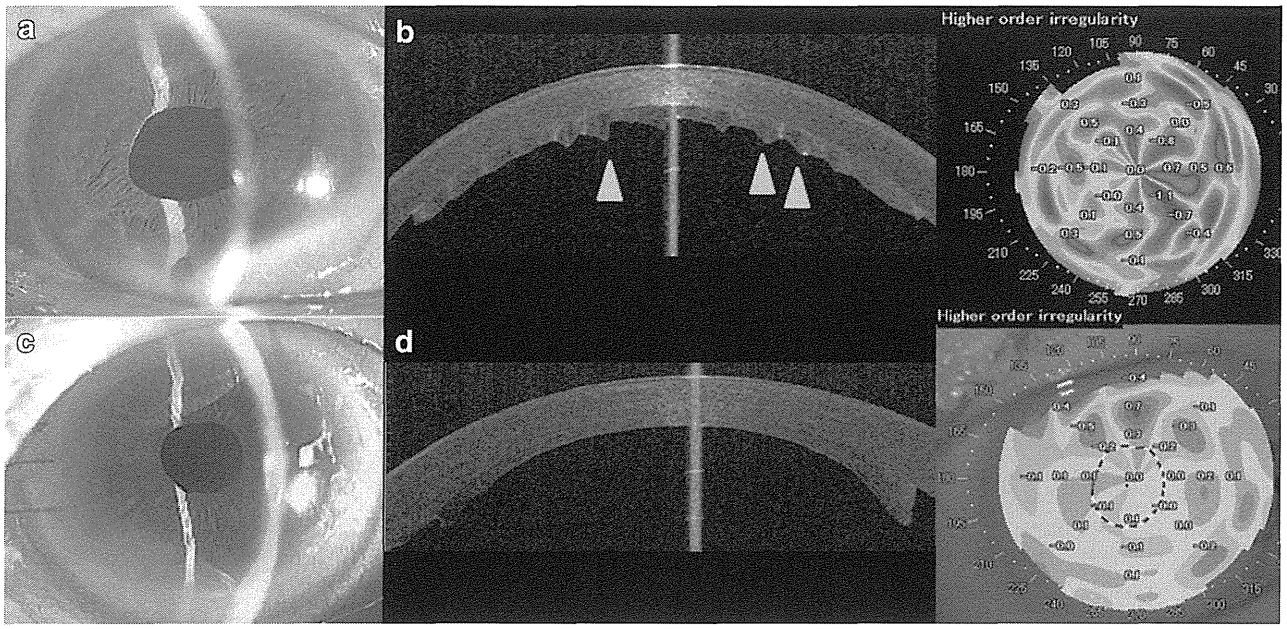

Fig. 1 Representative topography after f-DSAEK and m-DSAEK. Representative f-DSAEK cases (**a–b**: *upper row*) and m-DSAEK cases (**c–d**: *lower row*). Slit-lamp microscopy with clear transparent cornea after DSAEK in both treatment groups (*left column*). The AS-OCT images show the difference in the smoothness of the posterior surface of the grafts. In eyes after f-DSAEK, the wavy posterior surface was noted, especially in the center of the graft (**b**: *yellow arrow heads*), whereas the posterior surface was smooth in eyes after m-DSAEK. Fourier analysis of the total corneal dioptric power (anterior + posterior) demonstrated increased irregular astigmatism (*right column*) following f-DSAEK compared to m-DSAEK

and demonstrated that the irregularity was greater after f-DSAEK than after m-DSAEK and that visual acuity was poorer after f-DSAEK [27]. However, they evaluated only the x–z plane of the posterior surface, and optical data were not calculated for the anterior surface and total cornea. In the present study, both regular and irregular astigmatism optical data were analyzed using 3D Fourier analysis. Interestingly, the irregularity of the posterior surface of the f-DSAEK graft led to increased higher-order astigmatism and poor visual acuity. HOAs are an important cause of poor visual acuity after conventional DSAEK [9, 10]. As previously reported, the HOAs of the anterior, not the posterior, surface affect visual acuity because the difference in the refractive index of the anterior surface is much larger than that of the posterior surface [9, 10, 30]. However, our results indicate that, although the effect of irregular astigmatism in the posterior surface is theoretically small, the posterior surface can degrade the quality of vision when the irregularity is large, as seen with f-DSAEK.

Table 5 Endothelial cell density

	f-DSAEK	m-DSAEK	*P* value
Graft	2704 ± 677	2660 ± 285	0.78
3 months	1220 ± 467	1526 ± 489	0.81
6 months	1418 ± 530	1514 ± 579	0.96

Cells/mm^2

We postulate that the posterior side of the donor graft may become wavy from indentation during laser cutting or laser-induced lamellar roughness of the surface due to deep ablation. If the anterior corneal surface is compressed with too much force during fs-laser emission while the cornea is fixed at the peripheral sclera, wrinkles could form on the posterior surface of the graft, which would persist after decompression. Previous studies have also demonstrated that the surface of the stromal bed of a graft prepared with an fs-laser is rough compared to a microkeratome-prepared graft [31, 32], although the smoothness of the graft can also be affected by laser settings or swelling of the cornea [32].

Additional explanations for the poor visual outcome after f-DSAEK include interface scatter and the irregular posterior surface of the graft. Scatter is reported to degrade visual acuity after DSAEK [7]. Scatter after DSAEK might be related to corneal collagen denaturation due to the power of the fs-laser [32]. Collagen denaturation might become cicatrix and could cause scatter. The rough interface of the graft-recipient junction can cause scatter and degrade the quality of vision. In the present study, eyes with an irregular posterior surface after f-DSAEK had an irregular anterior surface compared to the m-DSAEK group. A comprehensive study that evaluates interface scatter, smoothness of the graft surface, and uniformity of the recipient stromal thickness is needed to address these issues.

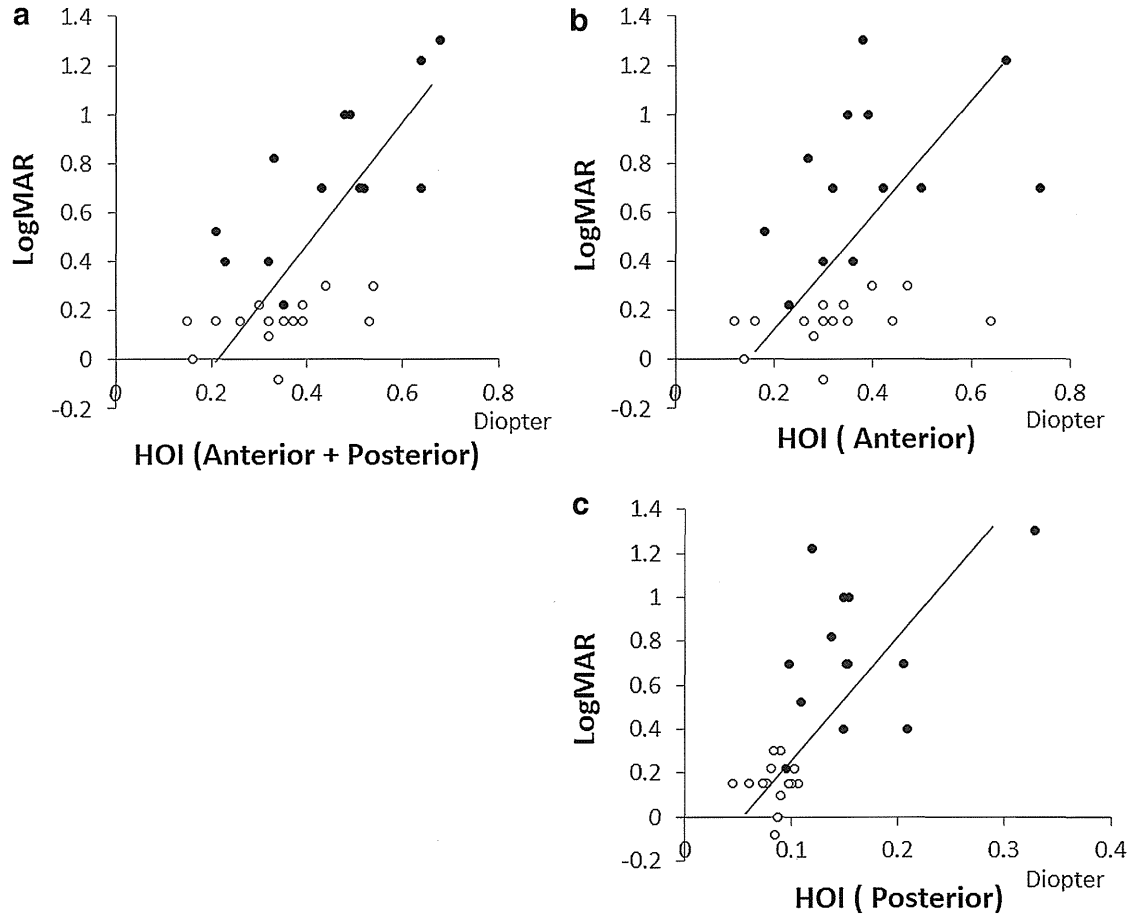

Fig. 2 Correlation between visual acuity and HOIs. Postoperative logMAR was significantly correlated with total HOI (**a**: anterior + posterior, $r = 0.6657$; $P < 0.001$), the HOI of the anterior (**b**: $r = 0.416$; $P = 0.016$,) and posterior surfaces (**c**: $r = 0.7064$; $P < 0.001$, respectively). The *open* and *closed circles* represent the data of m-DSAEK and f-DSAEK, respectively

In the current study, 9 eyes (36 %) after f-DSAEK and 3 eyes (17 %) after m-DSAEK showed graft dislocation and required air injections during the early postoperative periods. Although there was no statistical difference, the overall incidence of graft dislocation was relatively high after f-DSAEK. The incidence of graft dislocation after DSAEK varied among past reports, ranging from 2.1 to 26.5 % [3, 5]. However, Muftuoglu et al. showed that rebubbling after DSAEK did not have a statistically significant effect on mean corneal HOAs, although their study covered only a limited number of eyes [10]. Our study includes considerably more eyes that underwent rebubbling, especially after f-DSAEK, most likely because of the irregular thickness of the graft or the irregular interface of the graft as reported previously.

What measures can be taken to avoid the irregular posterior surface of f-DSAEK grafts and improve visual outcomes? First, graft preparation could be improved if preparation is observed by AS-OCT during fs-laser emission. Second, a curved surface on the fs-laser platform that fits the corneal curvature may prevent the formation of wrinkles during laser emission. Third, care should be taken not to let grafts fold during DSAEK surgery, especially when using thin f-DSAEK grafts. In our experience, we have observed folds or wrinkles in the graft immediately after air injection into the anterior chamber during DSAEK. The results of this study demonstrate that irregularity of the posterior surface of the cornea can degrade postoperative visual acuity.

In conclusion, the femtosecond laser has the potential to produce high-quality donor grafts for DSAEK. However, in this study, f-DSAEK produced more irregular astigmatism of the posterior surface than m-DSAEK, and irregularity of the posterior surface degraded optical quality, leading to a poor visual outcome.

Conflicts of interest D. Tomida, None; T. Yamaguchi, None; A. Ogawa, None; Y. Hirayama, None; S. Shimazaki-Den, None; Y. Satake, None; J. Shimazaki, None.

References

1. Price FW Jr., Price MO. Descemet's stripping with endothelial keratoplasty in 50 eyes: a refractive neutral corneal transplant. J Refract Surg. 2005;21:339–45.
2. Gorovoy MS. Descemet-stripping automated endothelial keratoplasty. Cornea. 2006;25:886–9.
3. Koenig SB, Covert DJ, Dupps WJ Jr., Meisler DM. Visual acuity, refractive error, and endothelial cell density 6 months after Descemet stripping and automated endothelial keratoplasty (DSAEK). Cornea. 2007;26:670–4.
4. Price MO, Gorovoy M, Price FW Jr., Benetz BA, Menegay HJ, Lass JH. Descemet's stripping automated endothelial keratoplasty: three-year graft and endothelial cell survival compared to penetrating keratoplasty. Ophthalmology. 2013;120:246–51.
5. Li JY, Terry MA, Goshe J, Shamie N, Davis-Boozer D. Graft rejection after Descemet's stripping automated endothelial keratoplasty: graft survival and endothelial cell loss. Ophthalmology. 2012;119:90–4.
6. Yamaguchi T, Negishi K, Yamaguchi K, Dogru M, Uchino Y, Shimmura S, et al. Comparison of anterior and posterior corneal surface irregularity in Descemet stripping automated endothelial keratoplasty and penetrating keratoplasty. Cornea. 2010;29:1086–90.
7. Patel SV, Baratz KH, Hodge DO, Maquire LJ, McLaren JW. The effect of corneal light scatter on vision after Descemet stripping with endothelial keratoplasty. Arch Ophthalmol. 2009;127:153–60.
8. Rudolph M, Laaser K, Bachmann BO, Cursiefen C, Epstein D, Kruse FE. Corneal higher-order aberrations after Descemet's membrane endothelial keratoplasty. Ophthalmology. 2012;119:528–35.
9. Yamaguchi T, Negishi K, Yamaguchi K, Murat D, Uchino Y, Shimmura S, et al. Effect of anterior and posterior corneal surface irregularity on vision after Descemet-stripping endothelial keratoplasty. J Cataract Refract Surg. 2009;35:688–94.
10. Muftuoglu O, Prasher P, Bowman RW, McCulley JP, Mootha VV. Corneal higher-order aberrations after Descemet's stripping automated endothelial keratoplasty. Ophthalmology. 2010;117:878–84.
11. Uchino Y, Shimmura S, Yamaguchi T, Kawakita T, Matsumoto Y, Negishi K, et al. Comparison of corneal thickness and haze in DSAEK and penetrating keratoplasty. Cornea. 2011;30:287–90.
12. Dubbelman M, Sicam VA, van der Heijde RG. The contribution of the posterior surface to the coma aberration of the human cornea. J Vis. 2007;7(10):1–8.
13. Yamaguchi T, Ohnuma K, Tomida D, Konomi K, Satake Y, Negishi K, et al. The contribution of the posterior surface to the corneal aberrations in eyes after keratoplasty. Invest Ophthalmol Vis Sci. 2011;52:6222–9.
14. Dickman MM, Cheng YY, Berendschot TT, van den Biggelaar FJ, Nuijts RM. Effects of graft thickness and asymmetry on visual gain and aberrations after Descemet stripping automated endothelial keratoplasty. JAMA Ophthalmol. 2013;131:737–44.
15. Kezirian GM, Stonecipher KG. Comparison of the IntraLase femtosecond laser and mechanical keratomes for laser in situ keratomileusis. J Cataract Refract Surg. 2004;30:804–11.
16. Kubaloglu A, Sari ES, Cinar Y, Cingu K, Koytak K, Coskun E, et al. Comparison of mechanical and femtosecond laser tunnel creation for intrastromal corneal ring segment implantation in keratoconus: prospective randomized clinical trial. J Cataract Refract Surg. 2011;36:1556–61.
17. Shousha MA, Yoo SH, Kymionis GD, Ide T, Feuer W, Carp CL, et al. Long-term results of femtosecond laser-assisted sutureless anterior lamellar keratoplasty. Ophthalmology. 2011;118:315–23.
18. Gaster RN, Dumitrascu O, Rabinowitz YS. Penetrating keratoplasty using femtosecond laser-enabled keratoplasty with zig-zag incisions versus a mechanical trephine in patients with keratoconus. Br J Ophthalmol. 2012;96:1195–9.
19. Shehadeh-Mashor R, Chan C, Yeung SN, Lichtinger A, Amiran M, Rootman DS. Long-term outcomes of femtosecond laser-assisted mushroom configuration deep anterior lamellar keratoplasty. Cornea. 2013;32:390–5.
20. Kymionis GD, Kontadakis GA, Grentzelos MA, Panagopoulou SI, Stojanovic N, Kankariya VP, et al. Thin-flap laser in situ keratomileusis with femtosecond-laser technology. J Cataract Refract Surg. 2013;39:1366–71.
21. Cheng YY, Hendrikse F, Pels E, Widjh RJ, van Cleynenbreugel H, Eggink CA, et al. Preliminary results of femtosecond laser-assisted Descemet stripping endothelial keratoplasty. Arch Ophthalmol. 2008;126:1351–6.
22. Heinzelmann S, Maier P, Bohringer D, Auw-Hadrich C, Reinhard T. Visual outcome and histological findings following femtosecond laser-assisted versus microkeratome-assisted DSAEK. Graefes Arch Clin Exp Ophthalmol. 2013;251:1979–85.
23. Kobayashi A, Yokogawa H, Sugiyama K. Descemet stripping with automated endothelial keratoplasty for bullous keratopathies secondary to argon laser iridotomy—preliminary results and usefulness of double-glide donor insertion technique. Cornea. 2008;27(Suppl 1):S62–9.
24. Tanabe T, Tomidokoro A, Samejima T, Miyata K, Sato M, Kaji Y, et al. Corneal regular and irregular astigmatism assessed by Fourier analysis of videokeratography data in normal and pathologic eyes. Ophthalmology. 2004;111:752–7.
25. Cheng YY, van den Berg TJ, Schouten JS, Pels E, Wijdh RJ, van Cleynenbreugel H, et al. Quality of vision after femtosecond laser-assisted descemet stripping endothelial keratoplasty and penetrating keratoplasty: a randomized, multicenter clinical trial. Am J Ophthalmol. 2011;152:556–66.
26. Rosa AM, Silva MF, Quadrado MJ, Costa E, Margues I, Murta JN. Femtosecond laser and microkeratome-assisted Descemet stripping endothelial keratoplasty: first clinical results. Br J Ophthalmol. 2013;97:1104–7.
27. Vetter JM, Butsch C, Faust M, Schimidtmann I, Hoffmann EM, Sekundo W, et al. Irregularity of the posterior corneal surface after curved interface femtosecond laser-assisted versus microkeratome-assisted Descemet stripping automated endothelial keratoplasty. Cornea. 2013;32:118–24.
28. Price MO, Price FW Jr. Descemet's stripping with endothelial keratoplasty: comparative outcomes with microkeratome-dissected and manually dissected donor tissue. Ophthalmology. 2006;113:1936–42.
29. Dapena I, Ham L, Melles GR. Endothelial keratoplasty: DSEK/DSAEK or DMEK–the thinner the better? Curr Opin Ophthalmol. 2009;20:299–307.
30. Hayashi T, Hirayama Y, Yamada N, Shimazaki-Den S, Shimazaki J. Descemet stripping automated endothelial keratoplasty for bullous keratopathy with an irregular posterior surface. Cornea. 2013;32:1183–8.
31. Mootha VV, Heck E, Verity SM, Lakshman N, Mufluoglu O, Bowman RW, et al. Comparative study of Descemet stripping automated endothelial keratoplasty donor preparation by Moria CBm microkeratome, Horizon microkeratome, and Intralase FS60. Cornea. 2011;30:320–4.
32. Rossi M, Misto R, Gatto C, Garimoldi P, Campanelli M, D'Amato Thothova J. Protective effects of deswelling on stromal collagen denaturation after a corneal femtosecond laser cut. Invest Ophthalmol Vis Sci. 2013;54:4148–57.

Global Consensus on Keratoconus and Ectatic Diseases

José A. P. Gomes, MD, PhD, Donald Tan, MD, PhD,† Christopher J. Rapuano, MD,‡ Michael W. Belin, MD,§ Renato Ambrósio, Jr, MD, PhD,¶ José L. Guell, MD,‖ François Malecaze, MD, PhD,** Kohji Nishida, MD,†† and Virender S. Sangwan, MD‡‡, the Group of Panelists for the Global Delphi Panel of Keratoconus and Ectatic Diseases*

Background: Despite extensive knowledge regarding the diagnosis and management of keratoconus and ectatic corneal diseases, many controversies still exist. For that reason, there is a need for current guidelines for the diagnosis and management of these conditions.

Purpose: This project aimed to reach consensus of ophthalmology experts from around the world regarding keratoconus and ectatic diseases, focusing on their definition, concepts, clinical management, and surgical treatments.

Methods: The Delphi method was followed with 3 questionnaire rounds and was complemented with a face-to-face meeting. Thirty-six panelists were involved and allocated to 1 of 3 panels: definition/diagnosis, nonsurgical management, or surgical treatment. The level of agreement considered for consensus was two thirds.

Results: Numerous agreements were generated in definitions, methods of diagnosing, and management of keratoconus and other ectatic diseases. Nonsurgical and surgical treatments for these conditions, including the use of corneal cross-linking and corneal transplantations, were presented in a stepwise approach. A flowchart describing a logical management sequence for keratoconus was created.

Conclusions: This project resulted in definitions, statements, and recommendations for the diagnosis and management of keratoconus and other ectatic diseases. It also provides an insight into the current worldwide treatment of these conditions.

Key Words: keratoconus, corneal ectasia, consensus, corneal cross-linking, corneal transplantation

(*Cornea* 2015;34:359–369)

Keratoconus and ectatic corneal diseases have been recognized for more than 150 years.[1,2] Over the last 2 decades, there has been a revolution in the knowledge related to the diagnosis and management of these conditions. In terms of diagnosis, the advent of corneal topography, and more recently corneal tomography, has increased the ability of ophthalmologists to identify corneal ectasia at a much earlier stage than was previously possible.[3] As a result, the previously established prevalence of keratoconus of approximately 1/2000 among the general population[4] has been challenged with much higher prevalence rates found in many parts of the world.[5,6]

The surgical treatment for keratoconus reflects this evolution.[7] Alternative procedures, such as the use of intrastromal corneal ring segment(s) (ICRS),[8,9] corneal cross-linking (CXL),[10–12] therapeutic excimer laser treatments including phototherapeutic keratectomy[13] and photorefractive

Received for publication January 8, 2015; revision received January 25, 2015; accepted January 26, 2015. Published online ahead of print March 2015.
From the *Department of Ophthalmology and Visual Sciences, Federal University of São Paulo/Escola Paulista de Medicina (UNIFESP/EPM), São Paulo, Brazil; †Cornea Service, Singapore National Eye Centre, Singapore, Singapore; ‡Cornea Service, Wills Eye Hospital, Philadelphia, PA; §Department of Ophthalmology and Vision Science, University of Arizona, Tucson, AZ; ¶Instituto de Olhos Renato Ambrósio, Rio de Janeiro, Brazil; ‖Department of Ophthalmology, Autonoma University of Barcelona, Barcelona, Spain; **Service d'Ophtalmologie, CHU Toulouse-Purpan, Toulouse, France; ††Department of Ophthalmology, Osaka University Medical School, Osaka, Japan; and ‡‡Center for Ocular Regeneration (CORE), L V Prasad Eye Institute, Hyderabad, India.
Supported by the Asia Cornea Society, The Cornea Society, EuCornea, and the Panamerican Cornea Society (PanCornea).
The authors have no conflicts of interest to disclose.
Study development and scientific support by Coordinators of the panels. Web portal development, conduction of statistical analyses, and medical writing support by Eurotrials, Scientific Consultants S.A. Coordinators who were involved in development of the round questionnaires, moderation of the panels, discussion of the round results, and writing of the manuscript (J.A.P.G., D.T., C.J.R., J.L.G., R.A., M.W.B., F.M., K.N., and V.S.). Panelists who were involved in the questionnaires responses and discussion at the face-to-face meeting in Chicago: Alaa El Danasoury, Aldo Caporossi, Beatrice Cochener, Choun-Ki Joo, Christopher R. Croasdale, Daniel H. Scorsetti, Deborah Jacobs, Denise de Freitas, Enrique Graue-Hernandez, Enzo Sarnicola, Farhad Hafezi, Friedrich Kruse, Florence Malet, George D. Kymionis, Gerard Sutton, Harminder S. Dua, Irving Raber, Jodbhir Mehta, Juan C. Abad, Luís Izquierdo Jr, Luis A. Rodriguez, Marian Macsai, Mauro SQ Campos, Naoyuki Maeda, Penny A. Asbell, Prema Padmanabhan, Rajesh Fogla, Richard Davidson, Robert Feder, Roberto G. Albertazzi, Samar Basak, Sheraz Daya, Shigeto Shimmura, Stephen Kaufman, Victor L. Perez, and Wolf Wonneberger.
Asia Cornea Society, Cornea Society, EuCornea, and PanCornea also contributed in both logistical support and in funding the face-to-face meeting in Chicago.
This project was primarily funded by an independent educational grant by the Asia Cornea Foundation. The funding body had no role in the design, implementation, or interpretation of the results of this project. This funding defrayed the cost of statistical analysis, 4 rounds of the Delphi Panels, printed materials, portfolio, supplements, questionnaires, and travel of coordinators of Eurotrials to the face-to-face meeting in Chicago. All the corneal societies contributed in both logistical support and also in funding the face-to-face meeting in Chicago and potential publication expenses.
Reprints: José A. P. Gomes, MD, PhD, Department of Ophthalmology and Visual Sciences, Federal University of Sao Paulo/Escola Paulista de Medicina (UNIFESP/EPM), R.São Paulo, SP, Brazil (e-mail: japgomes@uol.com.br).

keratectomy (PRK),[14] and phakic intraocular lenses (IOL)[15,16] alone or in combination[17–19] have been proposed to delay or even prevent the need for corneal transplantation. In addition, new techniques of keratoplasty have been developed such as deep anterior lamellar keratoplasty (DALK)[20,21] and femtosecond laser-assisted corneal transplantation.[22–24]

Although such advances have significantly improved our ability to diagnose and treat these patients, there remain many controversial aspects including disease definition and diagnosis and also medical and surgical management of these patients. These controversies have led to a need for achieving a consensus to assist practitioners in the management of patients with these conditions.

Formal consensus methods have become important tools to deal with complex problems in health care and medicine and to define levels of agreement on controversial topics.[25] They are also a powerful and logical way to generate current guidelines. One such tool is the Delphi method, which has been widely used in research in a variety of disciplines, including telecommunications, social sciences, and health sciences.[26–28] The goal of this technique is to obtain the most reliable consensus/level of agreement from a group of experts through an iterative process with several rounds of structured questioning.

The Delphi technique has been used in many fields of medicine including respiratory, cardiovascular, and neurological diseases.[29–31] In ophthalmology, the Delphi method has been used for establishing consensus on dry eye,[32] cataract surgery,[33] primary open-angle glaucoma,[34] thyroid eye disease,[35] infection prophylaxis,[36] age-related macular degeneration,[37] and ocular allergy.[38]

The current work presents a consensus regarding the management of keratoconus and other ectatic conditions from a panel of ophthalmology experts from around the world using a modified Delphi method. The consensus covers the most relevant and contentious questions regarding the definition, methods of diagnosis, and the nonsurgical and surgical treatments of these diseases.

METHODS

Design and Organization

We used a modified Delphi technique to obtain a consensus from an expert panel regarding important aspects of keratoconus and other ectatic diseases. One adaptation to this method was to include a face-to-face meeting to address unresolved issues after the initial question rounds (round 3) with a final presentation and approval by all panelists together (designated as Delphi +1).[32,38,39]

Each of the 4 supranational corneal societies, the Asia Cornea Society (Asia), Cornea Society (USA and international), EuCornea (Europe), and PanCornea (Latin America, the United States, and Canada), assigned 2 coordinators for the project (Asia assigned 1 additional coordinator—a total of 9 coordinators). These coordinators are accomplished cornea specialists with previous experience in the design, conduct, and publication of expert panels. Their role was: (1) literature review and identification of appropriate journal articles to send to the panelists, (2) design of methodology, (3) development of questionnaires, (4) selection of expert panel members, (5) decision-making process after each round, (6) writing the final manuscript, and (7) project oversight.

A Contract Research Organization (Eurotrials Scientific Consultants S.A., Lisbon, Portugal) provided methodological support during the rounds and was responsible for the data collection and statistical analysis.

Considering the multiplicity of themes, the coordinators formed 3 panels according to the following major topics of interest:

1. Definition/diagnosis: covering the clinical aspects that distinguish keratoconus from other ectatic diseases, diagnostic tests, and risk factors for keratoconus
2. Nonsurgical management: covering medical management and therapeutic approaches based on different scenarios
3. Surgical management: covering the factors or scenarios that lead to a particular surgical approach.

Selection of Expert Panel

Each Cornea Society compiled a list of potential participants complying with the following criteria:

1. Ophthalmologists with experience in the management of keratoconus and ectatic diseases
2. Authorship of scientific publications in high-impact medical journals
3. Wide recognition by the specialized medical community
4. Willing to comply with the initial question rounds, face-to-face meeting, and project timelines.

In addition, the pool of selected experts had to reflect a worldwide geographic distribution and had to equally represent the 4 corneal societies. Each society designated 9 experts, ensuring a total of 36 participants, plus coordinators, for this project.

An invitation e-mail was sent to the experts to explain the aim of the study, the major topic to be covered, the methodology, and to request their participation. In July 2014, the coordinators approved the group of selected experts and allocated 12 experts (3 from each society) to each major topic of interest (Fig. 1). All experts gave their consent to participate in this project.

Steps of the Process

The first 2 rounds of questionnaires were conducted between the August 1 and September 10, 2014. Before the first round, all experts were provided with the current literature regarding the diagnosis and management of ectatic diseases that included peer-reviewed research papers, systematic and narrative reviews, and editorials from recognized experts in the field. The method used to identify publications was to search electronic databases (Medline, EMBASE, and Cochrane Library) with the key words "*keratoconus, ectasia and ectatic corneal disease.*" The selection of articles was based on the relevance of the topic with novel information

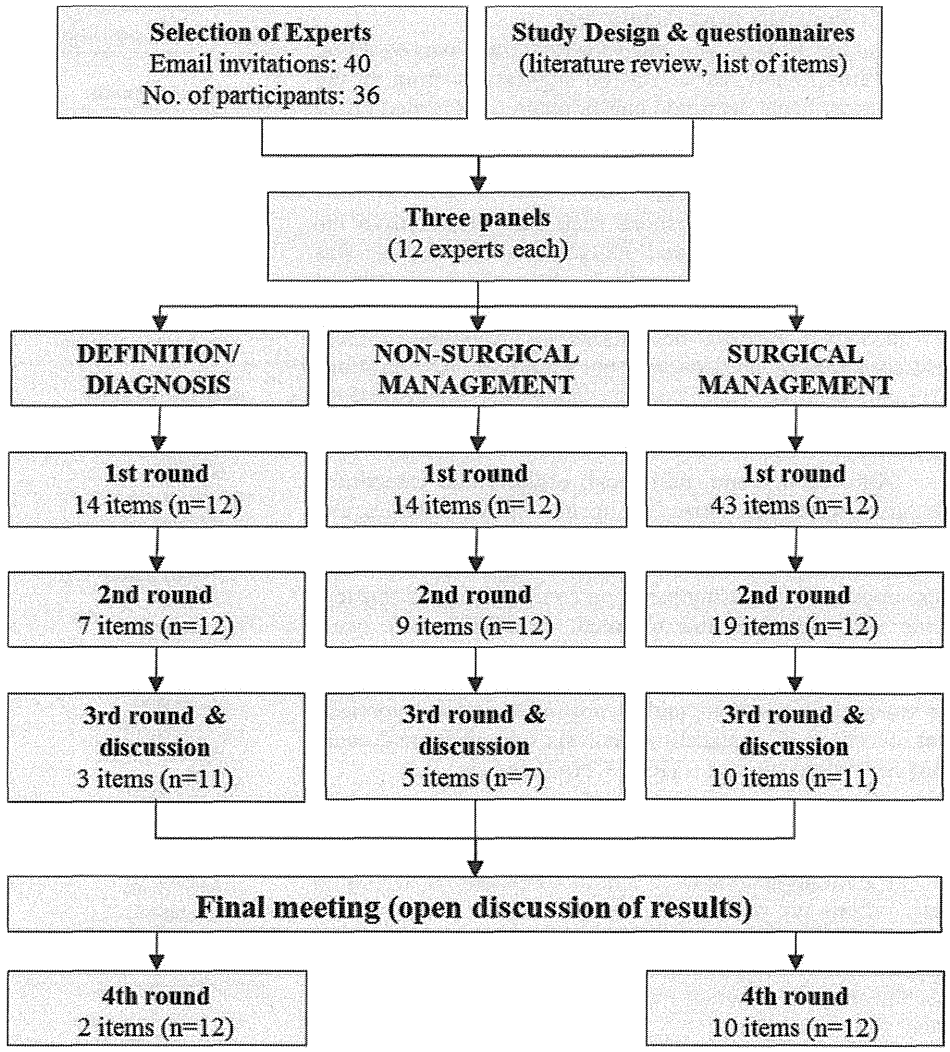

FIGURE 1. Flowchart of the project. No, number; n, number of participants.

that was not originally included in the major reviews by Krachmer et al and Rabinowitz.[1,2] To reduce attrition, a short turnaround time was selected and close follow-up was implemented, using personalized e-mails and regular reminders to nonresponding experts. To minimize the influence of seniority, presumptions of expertise, and dominant characters, the experts were kept anonymous from each other throughout the first 2 rounds.

A face-to-face meeting was held in Chicago on October 19, 2014, during the American Academy of Ophthalmology annual meeting. This meeting consisted of 3 modules:

1. Explanation of project rationale and methodology to be followed during the face-to-face meeting
2. Three panel sessions, according to the major topic. During these sessions, the results of the previous rounds were presented. In addition, the experts answered a third round of questions. The meeting was open to discussion, and when judged appropriate by all the experts, some items from previous rounds were revisited and subject to discussion. The inputs were registered and compiled. Each of these sessions was moderated by 3 coordinators who had no interference in the opinions or answers of the experts. One methodologist from Eurotrials ensured that each session complied with the defined procedures.
3. Final Meeting (Delphi +1), with open discussion involving all panelists and coordinators together to present and debate the results of the 3 panel sessions. Technically, this was accomplished by projecting the statements and revising them on screen until no more comments were raised from the participants. When found relevant by the majority of experts, unanswered controversial points were recorded. The coordinators then developed questions for one or more extra questionnaire rounds, which were sent back to the respective panel(s).

After the meeting and additional questionnaire rounds, the coordinators drafted a manuscript describing the results. The manuscript draft was circulated to all coordinators for their review and feedback. The manuscript was then revised incorporating all coordinators' feedback.

Data Collection and Analyses

The list of items generated for each topic was based on the literature review, as well as on suggestions from all the coordinators. Each electronic questionnaire was posted on an access-controlled Web site, and access credentials were distributed among participants. Only analysts had access to responses during the process.

The majority of questions seek a consensus from the experts regarding predefined statements. "Consensus" was considered when at least two thirds of the panel selected the same option. Other questions were aimed at understanding how the experts manage these diseases, considering different case scenarios (consensus was not required). All questions were closed-ended. Still, free text fields after each questions allowed the experts to write any comment if they felt necessary.

After each round, numerical, ordinal, and categorical responses were summarized using descriptive statistics and reviewed by the coordinators. Items on which consensus was not reached were reformulated into a new question. Items that were unclear or confusing based on comments in the free text fields were adjusted and repeated. Suggestions by panel members were incorporated.

Descriptive statistics were computed using percentages for categorical questions and means/medians for numerical/rank questions. The statistical analysis was performed using IBM SPSS Statistics 22.0 (IBM Corp, Chicago, IL).

RESULTS

E-mail invitations were sent to 40 experts, of whom 36 were willing to participate. The country distribution and subspecialties of the experts are shown in Table 1. Four persons declined to participate because of inability to attend the face-to-face meeting in Chicago (3) or because of financial reasons (1).

A 100% response rate was reached in the first 2 rounds in all the 3 panels. Twenty-nine of the 36 experts (80.5%) who answered the previous surveys attended the face-to-face meeting in Chicago: 11/12 in the Definition/diagnosis and Surgical management panels and 7/12 in the Nonsurgical management panel. During the Delphi +1 phase, the experts and coordinators concluded that a fourth round was necessary to rephrase or generate new questions regarding the Definition/diagnosis and Surgical management topics. This postmeeting round was conducted on-line from November 8 to December 18, 2014. The response rate during the fourth round of both Definition/diagnosis and Surgical management panels was 100% (Fig. 1). The items addressed throughout the rounds and during the face-to-face meeting and the consensuses obtained are hereby presented by their major topic.

TABLE 1. Coordinators and Expert Panel by Major Topic

Definition/Diagnosis	Nonsurgical Management	Surgical Management
Coordinators	Coordinators	Coordinators
Renato Ambrósio (Brazil)	José Gomes (Brazil)	José Guell (Spain)
Michael Belin (United States)	François Malecaze (France)	Christopher Rapuano (United States)
Kohji Nishida (Japan)	Virender Sangwan (India)	Donald Tan (Singapore)
Panelists	Panelists	Panelists
Juan Abad (Colombia)	Penny Asbell (United States)	Alaa El Danasoury (Saudi Arabia)
Roberto Albertazzi (Argentina)	Samar Basak (India)	Richard Davidson (United States)
Mauro Campos (Brazil)	Aldo Caporossi (Italy)	Sheraz Daya (United Kingdom)
Beatrice Cochener (France)	Denise de Freitas (Brazil)	Rajesh Fogla (India)
Christopher Croasdale (United States)	Farhad Hafezi (Switzerland)	Enrique Graue-Hernandez (Mexico)
Harminder Dua (United Kingdom)	Deborah Jacobs (United States)	Luís Izquierdo Jr (Peru)
Friedrich Kruse (Germany)	Choun-Ki Joo (Korea)	George Kymionis (Greece)
Robert Feder (United States)	Stephen Kaufman (United States)	Irving Raber (United States)
Marian Macsai (United States)	Florence Malet (France)	Luís Rodriguez (Venezuela)
Naoyuki Maeda (Japan)	Prema Padmanabhan (India)	Enzo Sarnicola (Italy)
Jodbhir Mehta (Singapore)	Victor Perez (United States)	Shigeto Shimmura (Japan)
Gerard Sutton (Australia)	Daniel Scorsetti (Argentina)	Wolf Wonneberger (Sweden)

Definition/Diagnosis

"Ectasia" as defined in most medical dictionaries refers to a dilation or distention of a tubular structure.[1] Historically, ophthalmologists, optometrists, and vision scientists have used this term broadly to cover many conditions associated with changes in the corneal shape. Although most of these ocular conditions do not meet the strict medical definition of ectasia, this panel will define ectasia by identifying which conditions should be classified under the term "ectatic disorder" and contrast these to other conditions that alter the corneal shape, but would not be considered a primary "ectatic disorder."

The first set of questions for the Definition/diagnosis panel aimed essentially to define and identify distinctive clinical characteristics of keratoconus when compared with other ectatic diseases. The experts agreed that abnormal posterior ectasia, abnormal corneal thickness distribution (eg, as seen with abnormal corneal thickness spatial distribution[40]), and clinical noninflammatory corneal thinning are mandatory findings to diagnose keratoconus. The exact values for any parameter will vary based on the machine being used and, for elevation values, the reference surface. Additionally, the values will vary if one is screening (eg, refractive surgery) where sensitivity is the overriding concern or treating (eg, cross-linking) where specificity assumes greater significance.

As opposed to a "thinning disorder," keratoconus, pellucid marginal degeneration (PMD), keratoglobus, and postrefractive surgery progressive corneal ectasia should be classified under

"ectatic diseases." Conditions such as Terrien marginal degeneration, dellen, and inflammatory melts should not be classified as ectatic diseases. Secondary changes (eg, posttrauma) where it is felt that no underlying ectatic propensity existed would be considered a "thinning disorder" as opposed to a primary ectatic disease. Consensus was achieved regarding the statements *"keratoglobus and keratoconus are different clinical entities"* and *"true unilateral keratoconus does not exist."* In addition, the *"thinning location and pattern"* are aspects that distinguish keratoconus, PMD, and keratoglobus.

The group also agreed that the best way to differentiate keratoconus from PMD is by using a combination of approaches, which includes a full corneal thickness map, slit-lamp examination, anterior curvature map and anterior tomographic elevation map. The group considered central pachymetry the least reliable indicator (or determinant) for diagnosing keratoconus because keratoconus can be present in a cornea of normal central thickness.

This panel also covered the criteria and the tests used to diagnose early or subclinical keratoconus. There was consensus that tomography (eg, Scheimpflug or optical coherence tomography) is currently the best and most widely available test to diagnose early keratoconus. Posterior corneal elevation abnormalities must be present to diagnose mild or subclinical keratoconus.

The group also intended to establish a classification for keratoconus. After 2 rounds and an extensive discussion on the topic, the group agreed that currently there is no clinically adequate classification system for keratoconus and that the historical Amsler–Krumeich classification fails to address current information and technological advances.[41] In the end, the panel felt it was beyond the scope of this project to create an entirely new keratoconus classification system.

The experts felt that there is no primary pathophysiologic explanation for keratoconus. During the face-to-face meeting, the panelists reached the conclusion that the pathophysiology of keratoconus is likely to include environmental, biomechanical, genetic, and biochemical disorders. Secondary induced ectasia may be caused by a purely mechanical process in a predisposed cornea, which may be unilateral. In addition, two relevant aspects were exhaustively debated: definition of ectasia progression and risk factors for keratoconus.

Definition of Ectasia Progression

Currently, there is no consistent or clear definition of ectasia progression. This led the Definition/diagnosis group to use 2 additional questionnaire rounds in an attempt to better define ectasia progression: "Ectasia progression" is defined by a consistent change in at least 2 of the following parameters where the magnitude of the change is above the normal noise of the testing system:

1. Steepening of the anterior corneal surface
2. Steepening of the posterior corneal surface
3. Thinning and/or an increase in the rate of corneal thickness change from the periphery to the thinnest point."

The changes need to be consistent over time and above the normal variability (ie, noise) of the measurement system (this will vary by system). Although progression is often accompanied by a decrease in best spectacle-corrected visual acuity (BSCVA), a change in both uncorrected visual acuity and BSCVA is not required to document progression. Although the panel agreed that specific quantitative data are lacking to further define progression and that these data would likely be machine/technology specific, it was agreed that the interval between testing/examinations should be shorter among younger patients and that the same measuring platform, when possible, should be used in sequential examinations.

Risk Factors

During the face-to-face meeting, the experts found it relevant to agree on the most important risk factors for keratoconus (an aspect that was not addressed during the previous rounds). Still, during the face-to-face meeting, no consensus was reached regarding this issue. Therefore, a postmeeting 4th questionnaire round was required involving the Definition/diagnosis panel to identify the relevant risk factors: Down syndrome, relatives of affected patients especially if they are young, ocular allergy, ethnic factors (eg, Asian and Arabian), mechanical factors, eg, eye rubbing, floppy eyelid syndrome, atopy, connective tissue disorders (Marfan syndrome), Ehlers–Danlos syndrome, and Leber congenital amaurosis. The consensuses reached by the Definition/diagnosis panel are summarized in Table 2.

Nonsurgical Management

Initially, the experts ranked the most important goals in the nonsurgical management of ectasia by the order of importance. However, during the face-to-face meeting, panelists agreed that the best approach was to select the 2 most important goals, which were halting disease progression and visual rehabilitation.

The level of importance of several measures used in the nonsurgical management of ectasia was graded by the panel. The most important measures were: verbal guidance to the patient regarding the importance of not rubbing one's eyes, use of topical antiallergic medication in patients with allergy, and use of topical lubricants (in case of ocular irritation) to decrease the impulse to rub one's eyes.

Experts agreed that in cases of allergy or if there is any allergic component, patients should be treated with topical antiallergic medication and lubricants. In addition, the group agreed that topical multiple-action antiallergic medications (ie, antihistamines, mast cell stabilizer, antiinflammatory) should be used in patients with keratoconus with atopy or history of eye rubbing.

During the first 2 rounds, there was disagreement about the relationship between keratoconus and dry eye. Therefore, the Nonsurgical management panel discussed the most appropriate way to define this relationship. The group agreed on the statement *"There is no direct relationship between keratoconus and dry eye."* Also, when discussing this topic, the group agreed with the statement *"Use of eye drops without preservatives is preferable in keratoconus patients."* All panelists recognized that preservative-free agents reduce irritation and epithelial trauma compared with agents with preservatives